A neurocomputational model of the basal ganglia for the analysis of motor deficits after dopaminergic loss in Parkinson's disease

Ilaria Gigi[1], Rosa Senatore[1], Angelo Marcelli[1]
[1]DIEM, University of Salerno, Via Giovanni Paolo II, 132, 84084 Fisciano, SA, Italy

Abstract

The basal ganglia (BG) are part of a basic feedback circuit, regulating cortical function, such as voluntary movement control, via their influence on thalamocortical projections. BG disorders, namely Parkinson's disease (PD), characterized by the loss of neurons in the substantia nigra (SN), involve the progressive loss of motor functions. The process that leads to these neural alterations is still unknown. At the present, PD cannot be cured, but an early diagnosis (ED) could allow to better manage its symptoms and evolution. A branch of neuroscience research is currently investigating the possibility of using motor alterations, e.g. handwriting, caused by the disease as diagnostic signs in the early stage of the disease, expression of small entity of SN lesion.

In the present work, we propose a neurocomputational model to investigate the behaviour of the simulated neural system after several degrees of lesion, with the aim of evaluating, if possible, which is the smallest lesion compromising motor learning. The performance of the network in learning a novel motor task has been analyzed, in physiological and pathological conditions. The proposed neural network proves that there may exist abnormalities of motor learning process, due to alterations in the BG, which do not yet involve the presence of symptoms typical of the confirmed diagnosis, since the network shows having some difficulties in motor learning already with 20% DA depletion.

Keywords — Basal ganglia, Motor learning, Neural networks, NEST, Parkinson's disease

1 Introduction

How do we choose between multiple competing responses and put the brakes on impulses? Which brain areas are involved in learning a novel behaviour, such as a motor task? What happens when a neurodegenerative disease affects the brain areas involved in executing a skilled task, such as a voluntary movement?

Deciphering the mechanisms by which brain structures support cognitive and motor functions is an important challenge for both the artificial intelligence (AI) and cognitive neuroscience communities; both investigate the processes that allow humans to efficiently perform reasoning and skilled movements, although from different perspectives. Based on a wealth of data, the basal ganglia (BG) are thought to play a principal role in this path.

Inspired by these concepts, the research presented in this article addresses the questions previously pointed out and aims at taking another step toward the analysis and understanding of the computational processes performed by the neural circuit of the BG using an AI approach.

The BG are subcortical nuclei part of several anatomical and functional loops, involving the cerebral cortex and the thalamus. They are involved in, among others, voluntary movements control, procedural learning, decision making, cognition and emotion. But the primary function is that of controlling and regulating the activities of the motor and premotor cortical areas for executing smooth movements after learning skilled responses to cortical inputs [1]. When systems-level interactions of multiple brain regions are involved, computational investigations provide a valuable complement to experimental brain research.

It is well established that the interactions between cortex and BG play an important role during learning. Here, these interactions have been investigated through a neurocomputational model that incorporates the key anatomical, physiological and biological features of these brain areas in an integrated functional network, based on accredited models in the literature. The aim of the model is to experimentally test the potential role of the BG in motor function, by means of open source and world-wide used tool in modern computational neuroscience, NEST. Exploration of the neural interactions could gain

some insights about the functional dynamics of information processing within the simulated brain areas, in normal as well as in diseased brains, providing also some guidelines for developing more efficacious therapies for many diseases in which these areas are involved.

In particular, BG dysfunction is associated with Parkinson's disease (PD), which is characterized by the loss of neurons in a region of the BG known as substantia nigra (SN). There is no accepted definitive biomarker of PD. An urgent need exists to develop early diagnostic biomarkers for two reasons: (1) to intervene at the onset of disease and (2) to monitor the progress of therapeutic interventions that may slow or stop the course of the disease.

A field of AI research deals with proving the existence of deteriorated behaviour in handwriting as the expression of a BG lesion of small entity, in the early stage of the disease. In this light, a neurocomputational model enables to investigate the behaviour of the simulated neural system after several degrees of lesion in order to evaluate which is the smallest lesion compromising motor learning. Such a lesion would represent a marker of the disease, existing before the onset of evident symptoms, as motor symptoms, which occur once the SN is severely damaged.

Therefore, the question is: is it possible to make an ED of the disease, even when the dopaminergic deficit is reduced and the motor symptoms are not yet evident? In other words, are motor learning deficits present early in the disease, when the motor deficits are not there yet? And if so, what characterizes deteriorated motor learning? Can these features be engineered, in order to develop support systems for assisting the clinicians to early diagnose the disease?

2 The basal ganglia model

The proposed model is based on the well-established neural networks and mathematical models developed (and widely cited in the literature) by prof. Michael J. Frank [2, 3], on the basis of electrophysiological and neuroanatomical studies, which incorporate the principal aspects of the BG anatomy and neurobiology, together with cellular and systems-level effects of DA. Frank's models are validated on Emergent, a tool that sets limits to the capability of both modeling and analysis of neural networks. In addition, recent studies have been considered, to support and refine the theoretical computational models of Frank, on one hand, and to instantiate the model in the motor learning domain for the experimental intent of the presented work.

In other words, the model here presented is a biologically plausible model of the BG, based on neuroanatomical studies and proven theoretical computational models; the main idea is that of encoding the behaviour of action selection of the BG as a *functional architecture*, going beyond the standard prevailing functional segregation of BG into 'direct' and 'indirect' pathways, thanks to the merging of several functional areas, as it will be explained in detail below.

The model is based on the following assumptions [2, 3]:

- Competitive dynamics between striatal cells in the direct and indirect pathways of the BG facilitate or suppress a given response. The cells that detect conditions to facilitate a response provide a *Go* signal, whereas those that suppress responses provide a *NoGo* signal.

- Dopamine (DA) has a key role in modulating the activity of the BG. Phasic changes in DA during error feedback are critical for learning stimulus-reward-response associations. Less DA leads to less contrast enhancement and impairs the ability to resolve Go/NoGo association differences needed for discriminating between subtly different responses.

- The STN provides a *Global NoGo* signal that suppresses all responses.

The BG circuitry incorporates the striatum, the globus pallidus (internal, GPi, and external segments, GPe), the subthalamic nucleus (STN) and the substantia nigra pars compacta (SNc) (Figure 1).

Depending on the input stimuli and past experience, the model selects a response through the interaction of distinct parallel subloops, each modulating a response. Particularly, each subloop comprises a direct (Go) and an indirect (NoGo) pathway for a given response. The direct pathway facilitates the response, whereas the indirect pathway suppresses the response. Therefore, competitive dynamics among subloops allow selective facilitation of one response with concurrent suppression of the others [2, 3].

Unlike models presented in the literature we have reviewed [1], which implemented them partially or do not explicitly report how they are implemented, the model we are presenting embodies all the following features, whose implementation details are also provided:

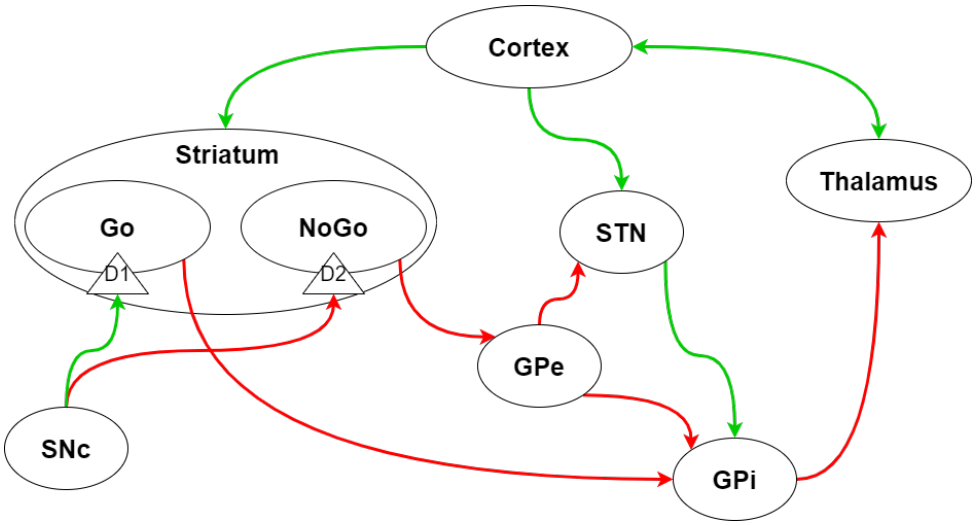

Figure 1: **The proposed basal ganglia model.** Schematic representation of the basal ganglia circuitry incorporated in the developed model. Red arrows represent inhibitory connections and green ones excitatory ones.

- The model includes the competing processes of the direct and indirect pathway and whether to gate (Go) or suppress (NoGo) a response is learnt.
- The model includes the SNc so that the role of DA can be implemented and manipulated, with simulated D1R and D2R in the striatum.
- The implementation of the model scales up Frank's model to include four competing responses, but can be extended proportionally to include more alternatives.
- The model does not include the prefrontal cortex (PFC) or maintenance of information over time, as the simulated tasks do not involve working memory. Instead, the cortical layer in the model is a simpler premotor cortex (PMC), representing the different responses.
- The model incorporates the subthalamic nucleus (STN) and thus allows to explore its contribution in providing a global modulatory signal on facilitation and suppression of all responses.
- The model implements STN dynamic effects, as response selection process evolves, both within the trial and with the advance of learning.
- The model take into account DA bursts and dips, with an increase of SNc unit firing for correct responses and a decrease to zero SNc firing for incorrect responses.
- The model simulates a learning rule based on a reinforcement learning paradigm inspired by the learning algorithm of Leabra [4], which, in short, is a combination of error-driven and Hebbian learning.
- The model incorporates the primary motor cortex (M1) itself to learn to favor a given response for a particular input stimulus, via Hebbian learning from the input layer.
- The model embodies the procedural motor learning hypothesis discussed in the Appendix A.1, allowing the BG to initially learn which response to gate via phasic changes in DA, ensuing from random cortical responses, and then this learning transfers to the cortex. In other words, BG and DA critically mediates the acquisition of a behaviour, but they play a diminishing role in executing well-learned behaviours.
- The model includes striatal interneurons for intrastriatal inhibition, as deduced from electrophysiological studies; they are included as functional structures, we have not included the heterogeneity and diversity of striatal GABAergic interneurons [1].
- Striatal interneurons are not modeled to undergo long-lasting modifications of the strength of synaptic transmission (LTP/LTD), rather synapses are constant.

- The model includes background activity of cortical and subcortical structures affected by external sources stimulation.

3 The proposed neural network

The neural network implementing the model comprises the circuitry of the BG presented in the previous section and the anatomical connections with the thalamus and MC, aiming at simulating the motor loop for learning and executing a motor behaviour. The architecture and dynamics are formally discussed in this section, whereas its behaviour is analyzed in the experiments. The scheme of the network is reported in Figure 2.

The model is implemented in NEST [5], currently one of the most used simulation tools in the modeling of large neuronal networks with biologically realistic connectivity. Unlike other simulators, such as Emergent [4], NEST allows to simulate large networks with a reduced computational cost and to simulate neuronal activation in a more realistic manner (for example, it allows to simulate multi-compartment neurons and particular types of synapses) and to set (and also measure) the firing rate of a population of neurons (Emergent only allows to know if a particular layer or neuron is active or not).

The adoption of NEST enables to drive an in-depth analysis, much more extensively than Emergent, and to simulate neuronal lesions to various degrees, acting on the firing rate of neurons rather than simulating only the presence/absence of a neuron; we are able to examine in details the behaviour of both the manipulated neuronal layers and all the other depending neuronal layers in terms of neuronal activity (i.e. firing rate).

The BG network here developed maintains proportional dimensional characteristics between neuronal layers, like in Frank's models, based on anatomical studies (Figure 2). In the light of this, the beneficial feature of NEST being able to simulate large neuronal population at a small computational cost, with regard to the other simulation tools, primarily translates into the chance to expand the model to consider, as enhancement, both wider neuronal populations (in terms of number of neurons in the network) and more complex behaviours. The latter, in particular, is meant both in terms of lower-level neuronal models (i.e. more biologically detailed) and of larger neural network models, including more brain structures, therefore more complex dynamics. From this perspective, the proposed model unwinds the binds of more comprehensive analysis by replacing the IF model with biologically more precise models, more computationally expensive but that take into account specific neuronal hallmarks. Also, given the growing use of NEST by neuroscience research, the network can be connected with little effort to other models in order to simulate more complex behaviours.

3.1 Architecture

The neural network implementing the BG model consists of a series of populations of neurons modeled as integrate-and-fire (IF) neurons (Appendix A.2. We are now going to describe the layers and their synaptic connections individually, to provide a general picture in a bottom-up approach.

Striatum In neurophysiology, direct (Go) and indirect (NoGo) pathways start from two distinct populations of neurons in the striatum, expressing D1 and D2 receptors, respectively. In the developed neural network, the four leftmost columns of the striatum represent the direct pathways, whereas the four rightmost columns represent the indirect pathways. Each column is involved in the selection/inhibition of a particular response, namely Response1, Response2, Response3, Response4. The Go columns project to the corresponding columns in the GPi, whereas the NoGo columns project to the corresponding column in the GPe. This is clear by Figure 2, in which an inhibitory connection starts from the Go columns coloured in teal and projects to GPi, while another connection is marked from NoGo area coloured in orange and projects to GPe. These connections are structured per columns, as indicated in the Figure 2 by the labels R1-R4 below the columns of GPi and GPe layers.

GPe GPe columns inhibit the associated columns in GPi, so that striatal Go and NoGo activity have opposing effects on the GPi. This concept is depicted in Figure 2 by the labels R1-R4 below the columns of GPi and GPe layers and the inhibitory connection between striatum-GPe-GPi, which represents the indirect pathway.

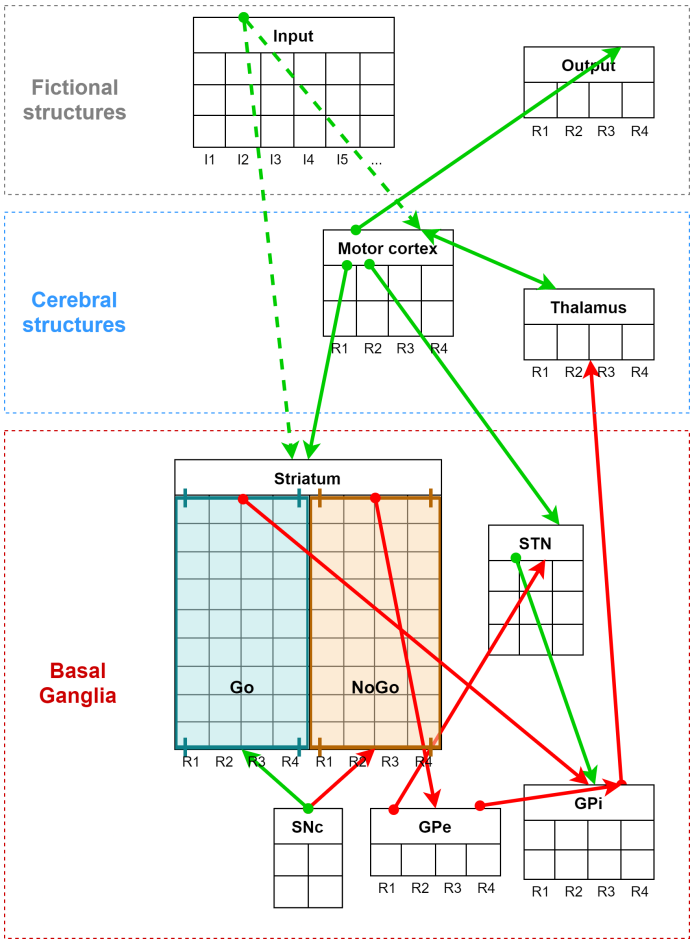

Figure 2: **The implemented neural network architecture.** The static architecture of the neural network, incorporating the basal ganglia nuclei in the red section (striatum, globus pallidus, substantia nigra, subthalamic nucleus), motor cortex and thalamus in the light blue section and some fictional structures in the grey section, necessary to produce (read) input (output) nervous stimuli. In green, excitatory connections; in red inhibitory connections; full line, fixed weight; dashed line, learning-dependent weight; in teal, Go columns of the striatum; in orange, NoGo columns. Squares represent units.

GPi Each column in the GPi tonically inhibits the associated column of the thalamus, which is reciprocally connected to the MC. This connection is depicted in Figure 2 by the labels R1-R4 below the columns of GPi, thalamus and MC layers and the connections between them. Thus, if Go activity is stronger than NoGo activity for a response, the corresponding column of the GPi will be suppressed, removing tonic inhibition of the corresponding thalamus unit, and eventually facilitating its execution in the MC. In other words, the direct pathway is implemented.

SNc Projections from the SNc to the striatum incorporate modulatory effects of DA. All the units of SNc excite Go columns (D1R) and inhibits NoGo columns (D2R).

STN The STN is beneficial for cognition in situations that would otherwise lead to "jumping the gun" on decision making processes, by preventing premature choices. This is achieved in the model by the excitatory projections from the STN to the GPi, representing the hyperdirect pathway.

The cortical layer in the model is a simple MC, representing just four different possible responses (although in principle it could be extended to include several responses). The thalamus layer is the reflection (in terms of columns) of the structure of the GPi, providing its role in the response selection process. The input and output layer are functional layers to provide input stimuli and read output stimuli from the neural network.

3.2 Neural Network dynamics, synaptic plasticity mechanisms and learning

Once described the static layers and synapses, it is possible to proceed with the analysis of the functional dynamics of the neural network.

According to the current knowledge [1] of the anatomical and physiological features of the BG, it has been suggested that different computational processes occur within this neural system, providing the learning ability that allows humans to acquire and accurately execute motor skills. In particular, the BG are specialized for reinforcement learning [2]; indeed, the BG nuclei receive the reward signal from the substantia nigra through the nigrostriatal dopaminergic projections. With regards to the role of dopamine (DA) as reward signal, it has been shown that phasic bursts and dips of DA occur during positive and negative feedback, respectively [2, 6].

Simulations start off with random weights, but the strength of the connections is reinforced or weakened during the course of training, depending on the feedback associated to the response selected by the network; in particular, representations in both the BG and cortical layers are learnt. This phenomenon allows the network to learn the stimulus–response (SR) associations needed to acquire and execute the motor task properly.

The simulation time, that is the time in which the behaviour of the network is analysed, is divided in two parts: the *minus phase* represents a response phase, in other words it is the time assigned to the network to choose a response, and the *plus phase* embodies a feedback phase, meaning that the mechanisms of reward and synaptic plasticity depend on the answer chosen in the minus phase. Each trial time contains a minus and a plus part of simulation, the minus phase lasts longer than the plus phase.

At the beginning of each trial, in the minus phase, a cortical input stimulus reaches the input nuclei of BG, giving rise to a sequence of neural activations within BG that leads to elicit a particular response. At the same time, the input stimulus directly activate multiple competing responses in the MC but these connections are not strong enough to select a response, therefore MC also needs support from the thalamus, whose activity is modulated by the BG. Nevertheless, at the beginning of learning, the connections which allow the disinhibition of thalamus to select a specific response through the Go columns, are very weak. Consequently, the BG, at first, do not select any response, rather it is randomly chosen; this behaviour depends on the background activity applied as Gaussian noise independently to the BG structures. In other words, the model "guesses" a response, ignoring whether it is correct or not.

The minus phase mimes the physiological dynamics: the network settles into activity states based on input stimuli and its synaptic weights, ultimately "choosing" a response; whereas the plus phase is purely fictional and is designed to represent the reward process, realized in a different way in the neurophysiology. For this purpose, the duration of the minus phase is set randomly variable: the network keeps running until the firing rate of one of the output neurons overpasses a threshold, as it means that one of the neurons is enough active in the time window to call it the answer of the network; if no answer reaches the threshold and the minus phase arrives at the maximum time limit, the most active neuron (i.e. the one with highest firing rate) is chosen.

Within BG network, there are four distinct subloops working in parallel, each modulating a particular response; therefore, selection is achieved by the interaction of these four distinct modules. In the plus phase, the activity of the SNc changes depending on the correctness of the response chosen by the network in the minus phase. Particularly, activity changes in the network according to the following criteria:

- Whenever the network selects the correct response, SNc activity increases (DA burst).
- Whenever the network selects the incorrect response, SNc activity decreases (DA dip).

As a result, striatal connection weights change depending on the difference between activity states of the network in the minus and plus phases and according to the learning rule. Whether there is LTP or LTD, the model is completely in the dark. Learning, in striatum, is deeply dependent upon the different striatal activation in the minus and plus phase: it causes LTP for a neuron x_i whether, in the plus phase, its activity is increased with respect to the minus phase and LTD otherwise. Instead, cortical learning follows Hebbian learning mechanism. Thus, the BG initially learns which response to gate via phasic changes in DA ensuing from random cortical responses; then, this learning transfers to the cortex once it starts to select the correct response more often than not [2]. The learning rates for striatal and cortical learning are chosen in a way that early in learning, striatal learning dominate, while later in learning, cortical learning predominates, according to the hypothesized motor learning theory (Appendix A.1).

Background noise All neuronal populations receive external excitatory synaptic input according to Poisson's distribution, to achieve realistic baseline firing rates and simulate background activity originating from stimuli from other brain structures not modeled. In particular, MC represents the main source of the excitatory input for striatum and STN and it is directly modeled in the neural network. Instead, it is known that the dopaminergic neurons fire spontaneously, providing tonic inhibition of downstream brain areas: this is achieved through a Poisson generator which excites the SNc. Similarly, baseline neuronal activation is modeled through the adoption of a Poisson generator for STN, GPi, GPe, MC. In particular, the MC is excited in the model by the input layer, but it has been shown by other neurophysiology studies [1] that it is stimulated by many other cortical areas (classically the visual cortex via the dorsal stream pathways, but also auditory, somatosensory and gustatory inputs); consequently the MC is highly active. Dopamine modulation has been structured as a rate-variable Poisson generator too.

Interneurons As already mentioned, Emergent allows to turn on/off single neurons and set elecrophysiological parameters for each neuron. It can also selectively switch off a percentage of neurons in a layer by setting parameters inside the layer. And this is how intrastriatal inhibition is modeled in Frank's models. Clearly, this implementation is far off the neurophisiology and difficult to manipulate. Besides, electrophysiological studies point out that interneurons are responsible for a tonic inhibitory activity in the striatum and are critical for shaping neuronal circuit activity in the striatum, particularly for modulating the activity of medium-sized spiny neurons (MSNs).

For this reason, we consider that to explicitly model interneurons as an additional functional module is essential. In our network, interneurons have been modeled as inhibitory connections among striatal neurons and we proved that the model shows the same behaviour of Frank's, although a totally different implementation of this aspect of the neurophysiology, as showed in the experiments.

STN dynamic effects As suggested by Frank [3], the STN provides a dynamic 'hold your horses' signal, temporarily preventing the execution of any response in face of high-conflict decisions. According to Frank's model, the STN would relay a global NoGo signal via excitatory projections to the pallidum with consequent inhibition of thalamocortical activity, thus allowing more time to integrate all necessary information and settle on the optimal choice. Based on investigations in healthy human subjects [7], the function of the 'hold your horses' signal may not be specific to complex decisional conflicts, but could generalize to basic sensorimotor functions in which preventing unwanted response is required. This model, known as 'proactive inhibition' assumes that inhibition over movement-triggering processes is maintained as long as the uncertainty lasts and releases the brake when appropriate, even for low-conflict decisions. The difference between the two models is subtle but the underlying hypotheses is the same (in particular, the former model assumes a phasic, reactive inhibitory process, whereas the latter rather refers to a tonic, proactive inhibitory process). This dissimilarity does not affect the developed model because the network is simulated under continuous stimuli, then the submitted implementation do not actually select one of the two theories.

Frank also points out that the simulations of his model revealed that this global modulatory signal could not be replaced by a simple response threshold parameter, because its effects are dynamic as response selection processes evolve [3].

In the developed neural network, as in [3], the influence of STN on other network layers and on the learning process is taken into account, hence the synapse connecting to GPi has been strengthened. Furthermore, the dynamic global function of the 'hold your horses' has been implemented by providing an excitatory random stimulus to the STN module through a Poisson generator, whose parameters dynamically change both as a function of *intra-trial* time (i.e. the simulation time of the minus phase) and *inter-trial* (i.e. from one trial to another). In order to compose appropriate functions, the dynamical connections to the STN have been observed through targeted simulations, to understand the net weight of all the efferent projections with the progress of response selection learning. From this analysis it was clear that both rate and weight of the Poisson generator had to drop according to an exponential law. Through an accurate analytical study, the parameters of the functions have been assessed and are reported in the Table 7. The designed exponential decay law for rate is reported in the Equation 1, while the law for weight in the Equation 2:

$$\begin{aligned} g(t) &= rate_f + (rate_i - rate_f) * e^{-\frac{t-t_i}{\tau_{rate}}} \\ \tau_{rate} &= \frac{t_f - t_i}{4 * \ln(2)} \end{aligned} \tag{1}$$

$$
\begin{aligned}
w(x,t) &= w_f + (w_i - w_f) * e^{-\frac{x}{\tau_w(t)}} \\
\tau_w(t) &= \tau_{intra} * c(t) \\
c(t) &= c_f + (c_i - c_f) * e^{-\frac{t-t_i}{\tau_{inter}}}
\end{aligned}
\tag{2}
$$

where $g(t)$ represents the decay law of STN firing rate, depending on inter-trial time, $w(x)$ represents the decay law of the weight and is depending on both intra-trial time and inter-trial time in the time constant, which decreaseas according to the decay law described by $c(t)$, which is function of inter-trial time.

The parameterized functions are plotted in the Figure 3.

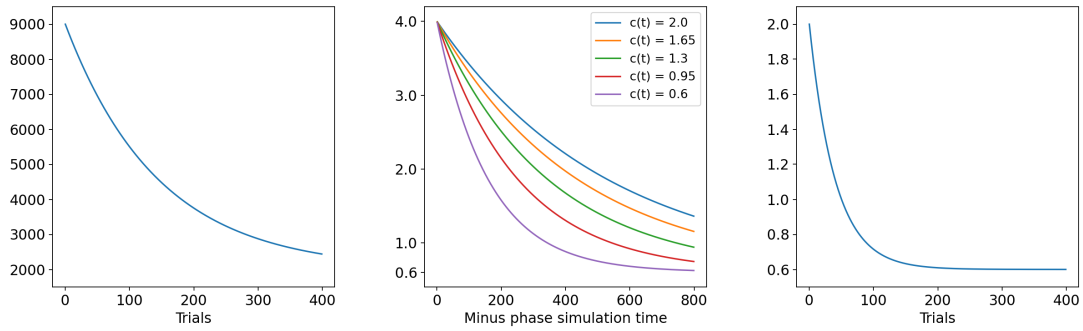

(a) (b) (c)

Figure 3: **STN exponential decay laws.** (a) The decay law for rate parameter. (b) The decay law for weight parameter, which depends both on intra-trial time and inter-trial time; c(t) is the function which regulates the intra-trial time constant according to inter-trial time. In blue the law for the initial value of c(t), in purple the final value; orange, green and red curves, in decreasing order, illustrate intermediate values of c(t). (c) Inter-trial decay law aimed at decreasing the intra-trial time constant depending on the inter-trial time.

3.3 Network parameter selection

The network parameters are obtained from the associated biological values through a process of normalization, as in [2, 3, 8].

The neurons of the network are modeled as IF; the main criterion for choosing the neuronal model has been to maintain a high level of abstraction, considered the complexity of the neuronal network, keeping the door open for potential more detailed analysis using a different model. Instead, the network structural and functional parameters represented a demanding and challenging job. The final values of the network parameters, the ones used in the experiments, are reported in Appendix A.4.

The size of the layers have been chosen according to Frank's models [2, 3], as already explained; in particular, adopting the dimensions of the model implemented in Emergent but choosing of encoding four different responses to be learnt and the inclusion of the STN. Clearly, it is an extreme computational schematization of the neurophysiology (for example, mouse striatum consists of around 1.7 million neurons), necessary to make simulations feasible. Other computational models, aiming at investigating synchronization and oscillations in neuronal populations require plausible details on synaptic dynamics and neuron behaviour, and then necessitate larger size; for example Lindahl and Kotaleski's network size is 80000 neurons, 70000 only in the striatum [9].

After, the synapses have been analysed, comparing the ones implemented in Frank's models and the ones offered by NEST. An initial parameter scenario has been chosen, based on Frank's models and physiological considerations, choosing to adopt static synapses (excitatory or inhibitory) and implementing them according to the neurophysiology. In particular, the weights of the synapses have been numerically hypothesized and then empirically investigated by repeated simulations. Once the functional aspects of the model have been implemented, other hyper-parameters have come into the play of refinement; inter alia, time windows, learning rates, thresholds and rates of generators.

It is necessary to introduce the physiological meaning (and how it translates into a computational model) of some important concepts commonly used for the statistical description of neuronal activity, which, in turn, encode the key parameters of the implemented neural network.

Firing rate First of all, *spiking activity* refers to the neural activity oscillations observed as a spike train (rhythmic patterns of action potentials called spikes). It is an important parameter in neural network model because local interactions between neurons can result in the synchronization of spiking activity. A plot of spiking activity is made of dots, each dot representing an individual action potential within the population of neurons, in order to determine what is the role of individual neural oscillations inside a network model. A commonly used measure of the spiking activity is the *firing rate*, generally defined as a temporal average in a trial k (i.e. mean firing rate) of the spike count n_k^{sp} in time window of duration T: $\nu_k = \frac{n_k^{sp}}{T}$. To get sensible averages, several spikes should occur within the time window. Typical values for the time window range from 100 ms to 500 ms. In this temporal interval, a task should be fully processed in the neural system considered. Clearly, in order to get a statistically significant parameter, the same experiment must be repeated several times to obtain adequate statistical power, since the measured spike count varies across trials [10, 11]. The firing rate, or rather the threshold by which the network selects the response in the time window, is crucial in the BG neural network for the evaluation of the network response.

Time window The *time window* for the evaluation of the spiking activity as the latency of the average firing rate for the BG model, particularly of MC and striatum is generally from 50 ms to 100 ms [12, 13, 11].

Learning rate The behaviour of the network, as expected, was found to be sensitive to the ratio of the striatal-nigral *learning rate*, which has to be set reasonably low. In short, as explained in details in Appendix A.3, the network behaviour initially depends more on the striatal-nigral learning and, later in training, depends more on the cortical learning. To obtain this condition, the cortical learning rate must be set small enough with respect to the striatal learning rate and the amount of weight variation derived from the activations in the striatum. It goes without saying that it has to be manually tuned. With regard to striatal reinforcement learning, the Hebbian term has a very low burden on the law and it is chosen according to [2], while the learning rate parameter of the whole law is chosen from 0.01 to 0.2.

Apart from structural and functional parameters, there are the parameters related to NEST generators (reported in Table 4), which also represent hyper-parameters of the proposed network. They have been chosen and gradually refined to reproduce the background activity behaviour simulated in [2, 3]. As starting point, frequency values suggested in the literature have been evaluated [14, 15].

3.3.1 Robustness analysis

The criterion leading the exploration of the space of parameters has been the aim of reproducing the physiological behaviour of BG model, sticking with the limitations of a computational model, which emerged from the analysis of the Frank's models implementation in Emergent, but exploiting the different and promising features offered by NEST.

Frank's network parameters have been chosen, which are based on neurophysiological measurements, then some of them have been adjusted, given the difference between the neuronal models adopted in this network and Frank's, to obtain the closest possible match to Frank's behaviour. Therefore, the parameter selection has been carried out by incrementally complex simulations, analysing first-hand the behaviour from the GUI until the required behaviour is achieved, which is needed to be fairly stable and suitably similar to the physiological behaviour feasible by a simulation tool. The next step, has been to conduct a robustness analysis, taking into account the background activity and variability that are inherent into the implementation to analyse the steady-state behaviour of the network (i.e. robustness of the model). Therefore, given small perturbations of the parameters, it is hypothesized that the general behaviour of the network remains unchanged and the dynamic reaches the steady-state with different transient regimes; in other words, the approach has been to explore the boundary conditions of all the parameters.

The robustness analysis has been divided into two branches: one for the *structural parameters*, the other for the *functional parameters*. With regard to the validated parameters contained in the Appendix A.4, the structural parameters are the synapses weights (Table 3), whereas the functional parameters are the ones in the Tables 5–6. Due to existing resources and time constraints, one full simulation was executed for each altered parameter, as long as the model reached the convergence behaviour; if the

behaviour turned out diverging, more than one simulation has been performed to analyse it in greater detail.

3.3.2 Structural parameters

The perturbation of the structural parameters has been set at ±20 %, a substantial range, with the purpose of moving towards the boundary line of instability in order to evaluate smaller extent whether a perturbed parameter causes unsteadiness at steady-state and return to steadiness with a reduced change of that parameter.

The result of the analysis showed that the increase of +20 % of all the parameters led to different transient times but steadiness was preserved. Instead, significantly lowering the parameters, given several simulations for the same change, involved impairment of learning. In particular, the parameter which caused it was the one crucial for learning, that is to say the weight of the synapse between MC and thalamus. Indeed, the excitation provided by the MC to the thalamus is fundamental for the activation of the thalamus from the BG and, therefore, for the selection of the response by the BG. The experiment has been useful to experience first-hand and figure out the significance of each individual synapse inside the neural network and how all of them impacts the big picture. In turn, the experiment allowed to change and pick the final parameters of the model wisely: the parameters have been finely tuned to enhance the behaviour of the model as a whole, strengthening or weakening each single subsystem by skilfully adjusting single synapses.

3.3.3 Functional parameters

The perturbation of the functional parameters cannot be statically organised like the structural ones. Indeed, while it is quite a natural choice to explore a static range around structural parameters, the very same concept is meaningless for the functional parameters, since they encode the dynamical behaviour of the neural network and they are strongly based on electrophysiology.

The minimum and maximum time of simulation for the minus phase has been explored for ±100 ms, ±200 ms, since the interval 200–1000 ms is a valid total time for the BG neural network to activate the MC and ultimately succeed in choosing a response as already mentioned. The duration of the plus phase remained fixed at 200 ms because it is totally a fictional simulation needed only to evaluate striatal spiking activity after DA burst or dip, whilst the minus phase is the simulation of the physiological network behaviour. The threshold for the firing rate is the most model-dependent parameter and it is strongly based on first-hand analysis of the neural activations. In particular, the most crucial one is the time window for the response selection in the minus phase, dependent on the activations obtained in the output layer (which is merely fictional). The threshold was initially computed at 0.17 in a time window of 120 ms, which means 21 spikes. The time window itself was put at first to 120 ms because there were very few activations given all the other baseline parameters. Such a time window choice, nevertheless, is not consistent with physiology: therefore, it has been halved and aligned with the time windows involved in learning. In this light, the time window has been varied within the range 40–80 ms with a granularity of 10 ms. The firing rate threshold is strongly tied to the time window and it has been investigated in ±1 spikes/Tw to ±2 spikes/Tw. Lastly, the learning rates have been fluctuated from ±20 % to ±50 %.

As it might be expected, raising a lot the threshold and reducing the nigro-striatal learning rate it entails the failing of learning within the estimated epochs. Instead, the speculated variations of the time windows and temporal constraints of the minus phase did not affect learning.

In addition to the robustness analysis itself, the parameters have been heavily and continuously combed through during the development and the experimentation stages, in order to refine the behaviour of the model.

4 Experimental results

In order to validate the model, the behaviour of the network in executing a motor task was evaluated by a set of simulations. Particularly, the functions of motor loops, comprising the interactions among the BG and MC was investigated.

4.1 The motor task

The experiments involve the motor task shown in Figure 4, which consists in reaching an ordered sequence of points by selecting the appropriate sequence of motor commands. The network, fed on a sequence of

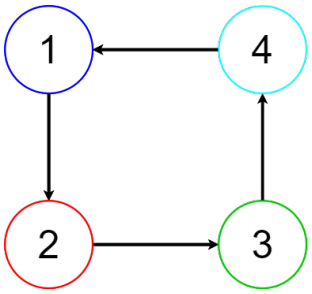

Figure 4: **Simulated motor task.** According to the input stimuli, representing the position of the current point, the network has to select the appropriate motor command to reach the next target point.

input stimuli, learns the correct SR associations which allow the model to complete the task selecting the appropriate motor command, at the appropriate time, within the sequence.

Therefore, after a certain number of training epochs, each consisting of four trials, the network learns the association and thus selects the correct sequence of motor commands to complete the task through the interaction of several modules within the BG circuitry.

4.2 Motor learning in physiological conditions

The network's job is to select either Response1 or Response2 or Response3 or Response4, depending on the task and the sensory input. At the beginning of each trial, incoming stimuli directly activate a response in the MC. However, these direct connections are not strong enough to elicit a robust response in and of themselves; they also require bottom-up support from the thalamus. The job of the BG is to integrate stimulus input with the dominant response selected by the MC, and on the basis of what it has learned in past experience, either facilitate (Go) or suppress (No-Go) that response.

Within the overall thalamocortical circuit, there are two parallel subloops that separately modulates the four responses, allowing the BG to *selectively* gate one response, while continuing to suppress the others. The striatum is functionally divided into two subpopulations. It must be pointed out that *left* and *right* column is referred to the neural network scheme in Figure 2, but in the raster plot they must be read from bottom to top, a neuron of each column distributed over eight. Striatal raster plots show the neuronal activations within a time window of 60 ms considered in the learning rule because they are the relevant ones for the purpose of learning. The four columns on the left are "Go" units for the four potential responses and simulate D1R. The four columns on the right are "NoGo" units and simulate D2R. Thus, the eight columns in the striatum represent "Go–Response1", "Go–Response2", "Go–Response3", "Go–Response4", "NoGo–Response1", "NoGo–Response2", "NoGo–Response3", "NoGo–Response4".

The Go columns project only to the corresponding column in the GPi (direct pathway), and the NoGo columns to the GPe (indirect pathway). The GPe columns inhibit the associated column in GPi, so that striatal Go and NoGo activity have opposing effects on the GPi. Finally, each column in the GPi tonically inhibits the associated column of the thalamus, which is reciprocally connected to the MC. Thus, if Go activity is stronger than NoGo activity for Response1, the left column of the GPi will be inhibited, removing tonic inhibition (i.e., disinhibiting) of the corresponding thalamic unit, and facilitating its execution in the MC. In the raster plot the columns must be read from bottom to top, precisely both MC and GPi column is represented by two neurons spaced by four.

At the beginning of training, random activity within the network causes the selection of a random answer. During learning the activity within each striatal column enables different Go and NoGo representations to develop for various stimulus configurations. In particular, the DA mechanism modulates striatal learning, since increases in DA during positive feedback lead to reinforcing the selected response, whereas decreases in DA during negative feedback lead to learning not to select that response.

After learning, the network has strengthened the correct Go/NoGo connections and is able to steadily complete the task.

4.2.1 Simulated motor learning task

The trials reported here are 0, 60, 100, 400, which correspond respectively to epoch 1st, 15th, 25th and 100th. Epoch 1st-15th can be considered the early stage of learning, epoch 25th represents the half stage and 100th the steady state after learning, knowledge extracted from Figure 21. Both epoch 1st and 15th

are considered because while the former corresponds to a fully random behaviour of the network, since parameters are randomly initialized, the latter shows the first traces of learning.

Early learning stage In the minus phase of the first epochs (recall one epoch corresponds to four trials), the GPi and GPe are massively activated due to the background neural activity; STN activity is influenced by the background neural activity and cortical afferents, exhibiting a light decay of the activations within the trial simulation; MC is strongly dependent on the random background activity and subsequently output activations, triggered by cortical activations, are random. The Figures 5–6 show how this behaviour is nearly the same both in trial 0 (1st epoch) and trial 60 (15th epoch) for the input/response 1, but since learning is advancing in trial 60 compared to trial 0, in which the behaviour is that of randomly initiated network without any hint of learning, in the 15th epoch first hints of the learning of Response1 are some *holes* in GPi activity, which mean that the effect of its afferents has changed, precisely of STN and striatum (Go). From Figure 5 (b) it can be noted that in the last 60 ms of the simulation (approximately half of the last time interval) the most active response (i.e: the response with the largest number of dots) is Response1, whereas in Figure 6 (b) it is Response4. These activations determine the response chosen by the network in the corresponding trial and cause a burst or dip of DA in the plus phase, namely, in the example being carried out, a burst if the response chosen is Response1, a dip otherwise.

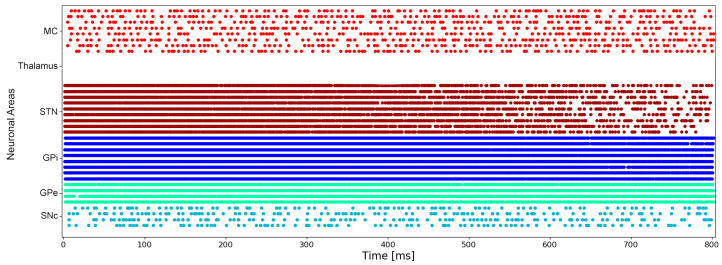

(a)

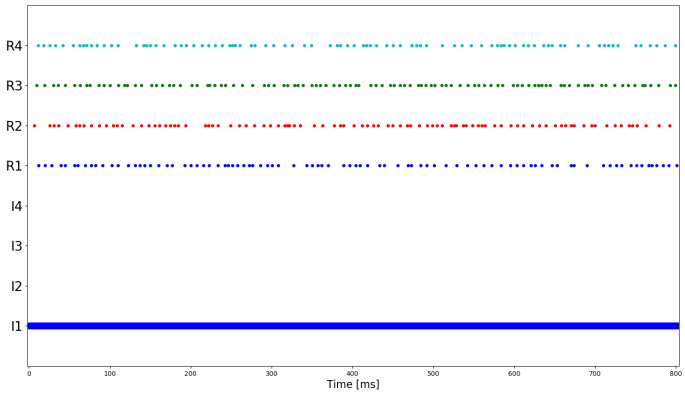

(b)

Figure 5: **Trial 0 minus phase (1).** (a) The network activations in the minus phase of trial 0. In red, cortical activations; in brown, STN activations; in blue, GPi activations; in green, GPe activations; in teal, SNc activations. Note that no activation in the thalamus occur at trial 0, which should be in pink. (b) Input/output activations. In trial 0, the input 1 is fed to the network; responses are randomly activated by MC activity.

At the beginning, striatal weights (in connection with Input) are not strong enough to disinhibit a column in the GPi to select a response, through the thalamus. Indeed, the thalamus is not active up to around the 100th trial. Actually, activations in the striatum are scarce, since they are triggered by the combined effects of tonic DA, Input stimulus and MC, whose major contribution is the one from Input, which is initially very low, see Figure 7. As learning advances, in the Figure 8 the initial randomly activated neurons of other columns than Go-Response 1 are being weakened in favour of neurons of Response 1. From Figure 8 it is clear that trial 60 is still to be considered in the early stage of learning, because activations, albeit increasing, are not enough to select the correct response.

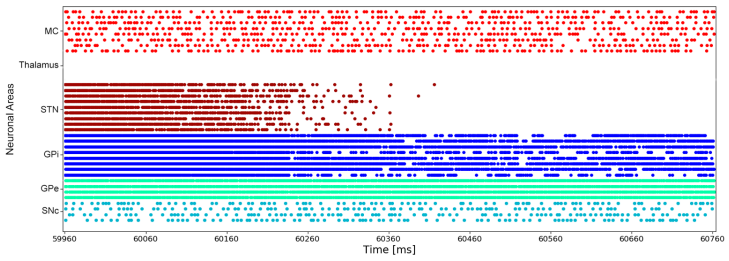

(a)

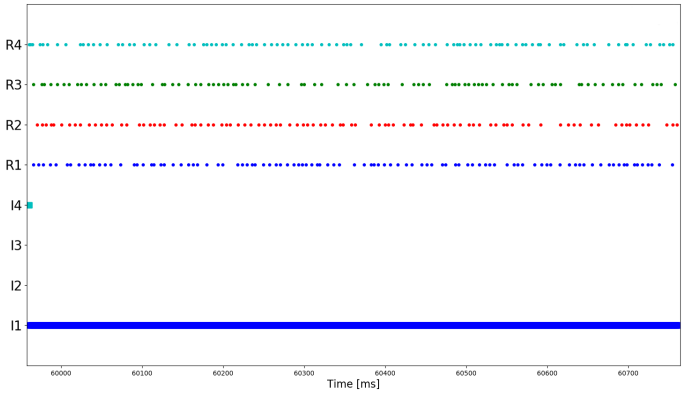

(b)

Figure 6: **Trial 60 minus phase (1).** (a) The network activations in the minus phase of trial 60. STN activity is high in the first half of the simulation time and goes to zero after. GPi activity is starting being inhibited by its afferents, a hint that learning is advancing. (b) Input/output activations. In trial 60, the input 1 is fed to the network; responses are still randomly activated by MC activity, since it is still an early stage of learning.

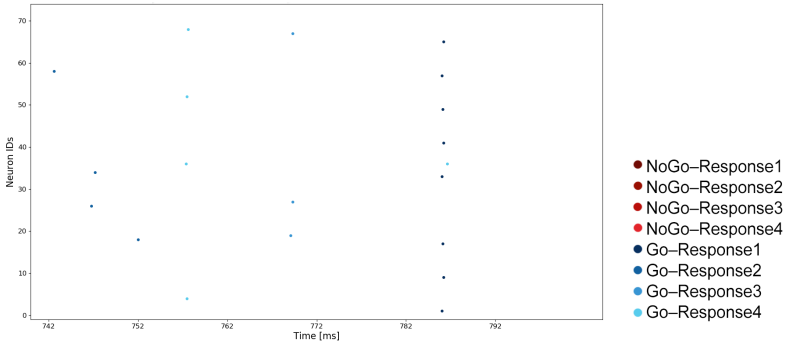

Figure 7: **Trial 0 minus phase (2).** Striatal activations in the minus phase of trial 0. striatum activity is weak and scarce; indeed, neurons in the Go columns randomly fire.

In the plus phase of trial 0 there has been a DA burst (Figure 9), appreciable from SNc activity, while in the one of trial 60 there has been a dip (Figure 10), indeed there is no nigral activity. Precisely, reading from bottom to top, neurons of the first column in MC are activated in Figure 9 (a), causing the activation of Response1 in Figure 9 (b). Conversely, in in Figure 10 (a) the column activated is the fourth, causing the activation of Response4 in Figure 10 (b). It is noteworthy that the dip of DA (Figure 10) causes the inhibition of the column corresponding to the answer chosen (Response4) in the GPe, due to the triggering of the indirect pathway for Response4, the last neuron from bottom to top. Instead, the burst of DA (Figure 9) activates the direct pathway, then it is expected the inhibition of Response1 column in the GPi, but it does not occur in trial 0 because the inhibitory effect is too weak at this stage.

The reward process is set in motion by the cortical activation of the response chosen and DA modulates the Go/NoGo activations, as already discussed. In this light, striatal activations in trial 0 show primarily Go column neurons of the corresponding response (that is Response 1 in this case, Figure 11, despite

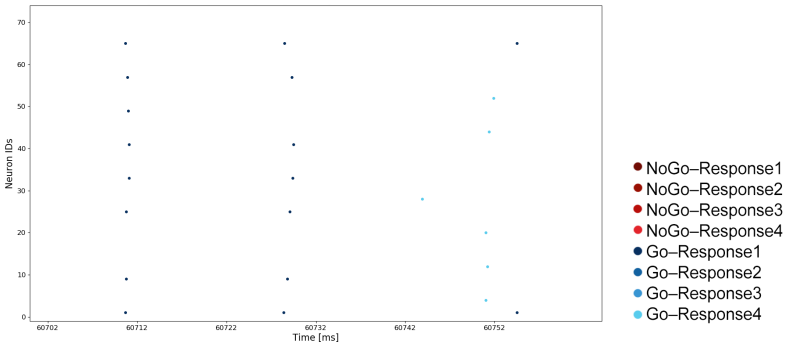

Figure 8: **Trial 60 minus phase (2).** Striatal activations in the minus phase of trial 60. striatum activity is still scarce, but it can be noted, with respect to Figure 7, that Go neurons for Response1 are a little more active and Go neurons for the other responses are being weakened.

there may be few activations of other Go neurons due to input effect, which do not cause LTP but reflect neuronal activation already present in the minus phase and rather, it is weakened. Note that the first Go activations are not so dense, but they will become denser with the advance of learning, thanks to the increased combined effect of Input and MC. Instead, striatal activity in trial 60 exhibits a dense activation of NoGo column neurons of Response4 (the one chosen in the minus phase, see Figure 10); this activity is not modulated by SNc but only by the MC. It is remarkable that all the single striatal neurons in the plus phase, although receiving the same stimuli for the reward process from MC, input and SNc, exhibit different activity in the simulation time: particularly not every neuron is being activated and they do not fire at the same rate. This effect is due to the inclusion of striatal interneurons.

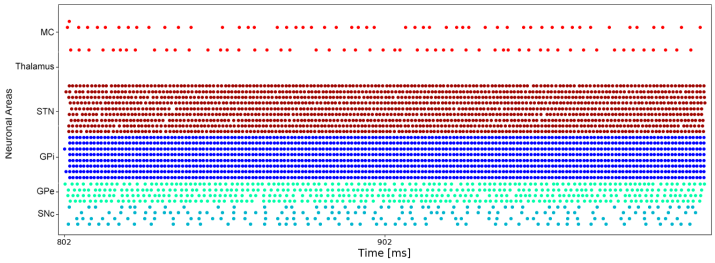

(a)

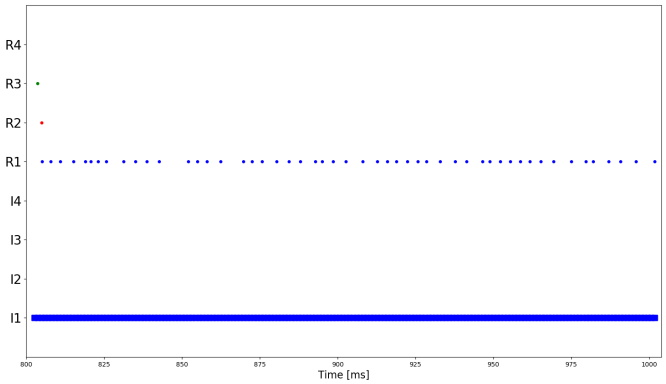

(b)

Figure 9: **Trial 0 plus phase (1).** (a) The network activations in the plus phase of trial 0. Nigral activations embody DA burst. (b) Input/output activations. The response chosen is correct.

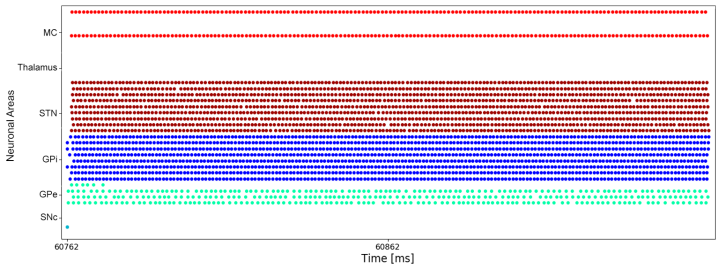

(a)

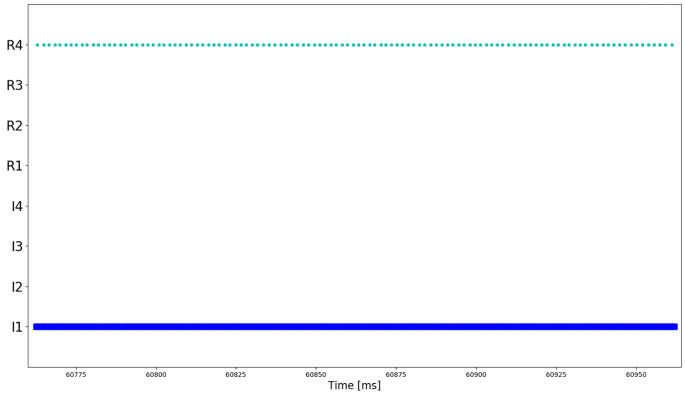

(b)

Figure 10: **Trial 60 plus phase (1).** (a) The network activations in the plus phase of trial 60. There is no activation in SNc: it represents a DA dip. (b) Input/output activations. The response chosen is incorrect.

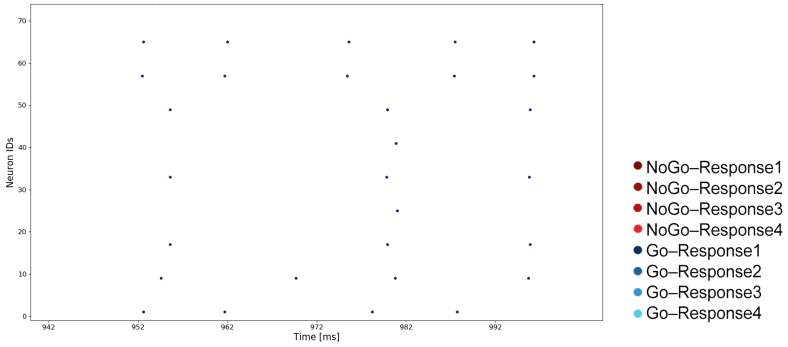

Figure 11: **Trial 0 plus phase (2).** Striatal activations in the plus phase of trial 0. Go-Response1 is primarily activated and causes LTP for the corresponding neurons and LTD for the neurons which are not represented here but were active in the minus phase (Figure 7).

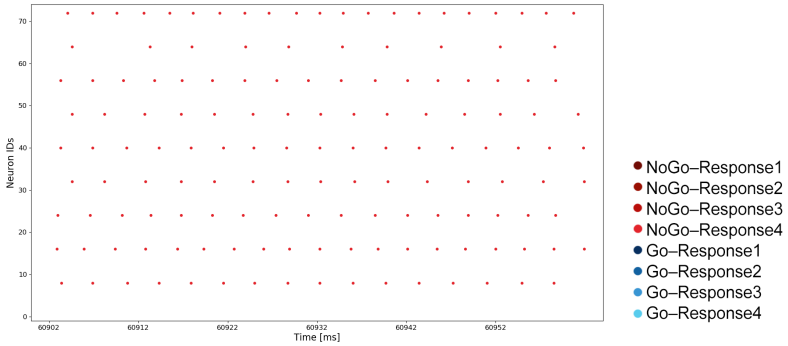

Figure 12: **Trial 60 plus phase (2).** Striatal activations in the plus phase of trial 60. NoGo-Response4 is activated and causes LTP for the corresponding neurons.

Half learning stage In the 25th epoch, striatal learnt weights are sufficient to inhibit GPi column corresponding to Response1 (the first neurons from bottom to top spaced by four), which lead to the disinhibition of the corresponding neuron in the thalamus, as shown in Figure 13 (a). The activation of the thalamus results in a visibly appreciable enhancement of Response1 (Figure 13 (b)). This time, the DA burst caused in the plus phase is because of BG, through the thalamus, and not by random cortical activity.

Striatal activations are enhanced with respect to the 1st-15th epochs, meaning that learning is proceeding for Response1 and the connection with the Input is being strengthened (Figure 14), although the network indecision is still reflected in activations for the other responses.

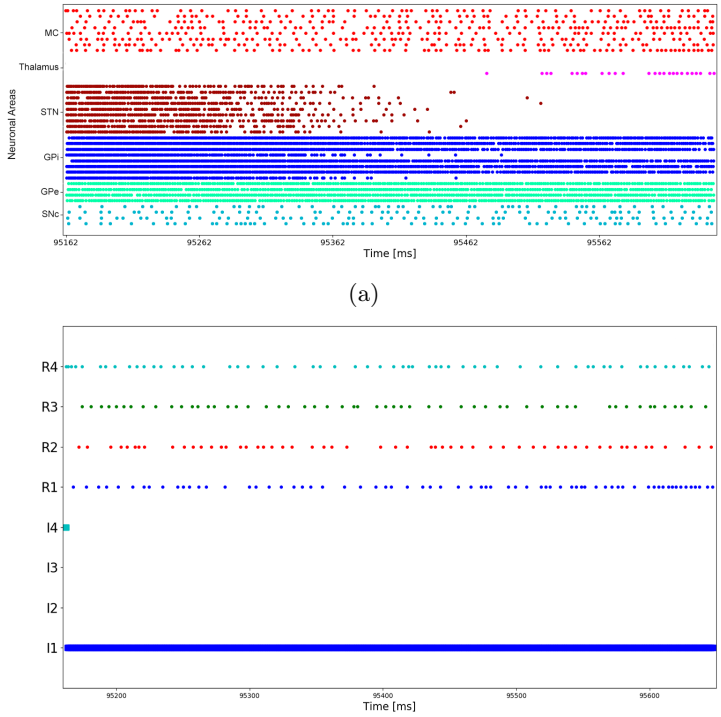

Figure 13: **Trial 100 minus phase (1).** (a) The network activations in the minus phase of trial 100. GPi column corresponding to Response1 is visibly inhibited, leading to a dense activation of the first neuron in the thalamus in the final section of the simulation. (b) Input/output activations. There is a visibly appreciable enhancement of Response1, which is then chosen in this trial.

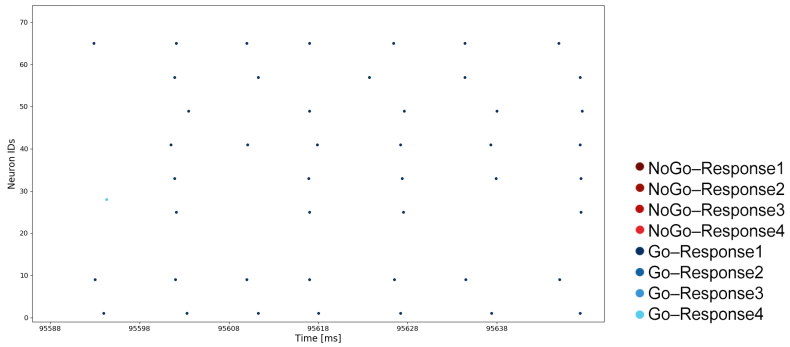

Figure 14: **Trial 100 minus phase (2).** Striatal activations in the minus phase of trial 100. Go-Response1 neurons are highly active and dominate the other columns, which are definitely weakened.

In the plus phase of trial 100 there has been a DA burst. The column in the GPi corresponding to Response1 is being inhibited, hint that Go striatal weights are being strengthened (Figures 15 and 16). It is also noticeable that cortical activity is increased: this is due both to cortical learning, which

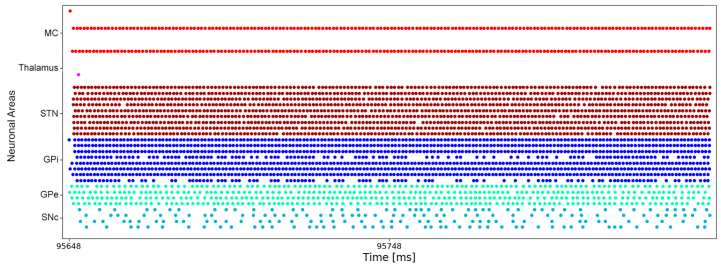

(a)

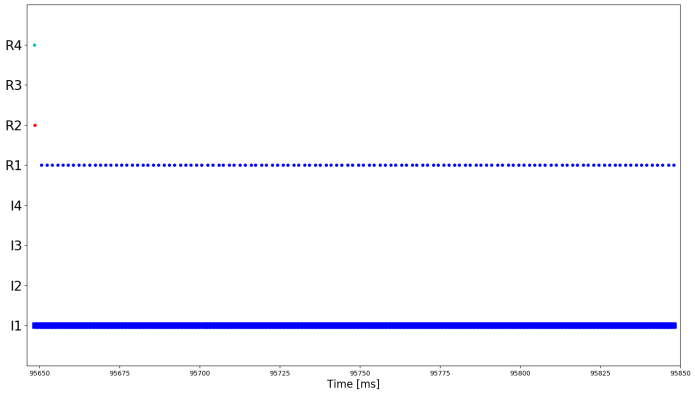

(b)

Figure 15: **Trial 100 plus phase (1).** (a) The network activations in the plus phase of trial 100. Clearly the response was correct and there is a DA burst. (b) Input/output activations. The response chosen is correct.

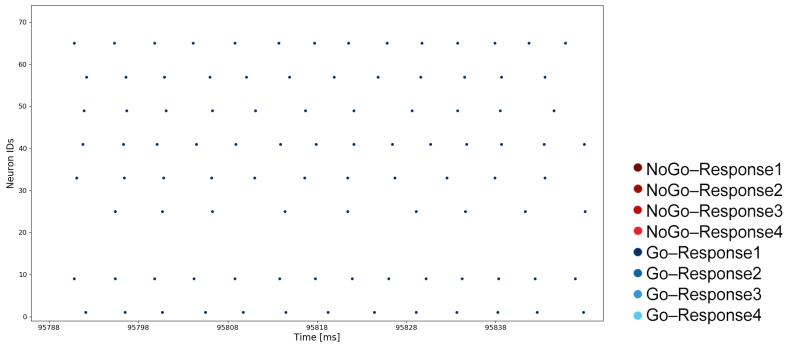

Figure 16: **Trial 100 plus phase (2).** Striatal activations in the plus phase of trial 100. The response is correct, then Go-Response1 is activated and causes LTP for the corresponding neurons. Note that the activations are more dense with respect to trial 0.

reinforces Input-MC connection, and the change in the pathway towards the thalamus, which, despite not sufficiently strong to activate the corresponding thalamic unit, still is being enhanced through striatal learning and ultimately assists to enhance MC activity.

Moreover, striatal activity of Go-Response1 neurons is clearly more dense than the activity observed in 1st-15th epochs. This behaviour, considering that phasic DA release is fixed, is due to the effect of the Input-striatum connection in the plus phase, which is being strengthened through learning.

Steady state after learning stage After learning, the network has learnt the correct SR associations for all the responses. This is clear in the example being carried out in this Section about Response1. Figure 17 (a) shows that the inhibition of the first column of the GPi is substantial and solid, as well as the activity in the thalamus. Also, activations of the first column in MC is robust. Consequently, in Figure 17 (b) the activation of the Response1 is visibly remarkable compared to the activations of the other neurons.

Secondly, striatal activations at steady state is massive for the correct response, Response1, and the other responses are correctly inhibited.

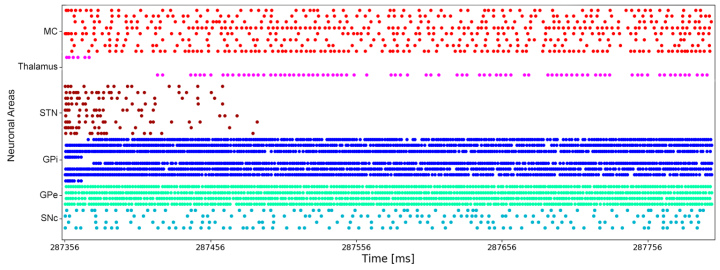

(a)

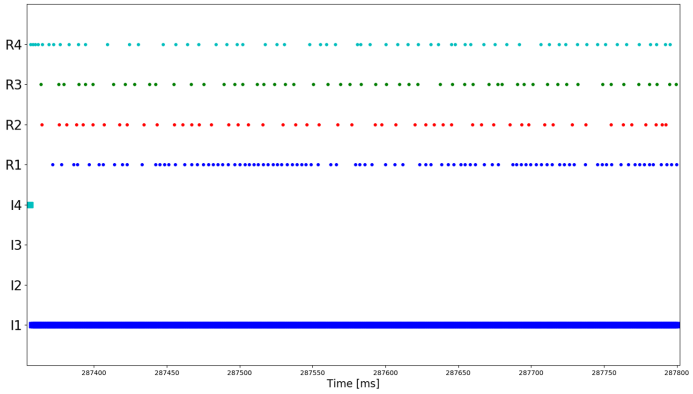

(b)

Figure 17: **Trial 400 minus phase (1).** (a) The network activations in the minus phase of trial 400. There are significant activations of first columns in MC and thalamus and solid inhibition of the first column of GPi, as expected. (b) Input/output activations. Response1 is clearly enhanced compared to the others.

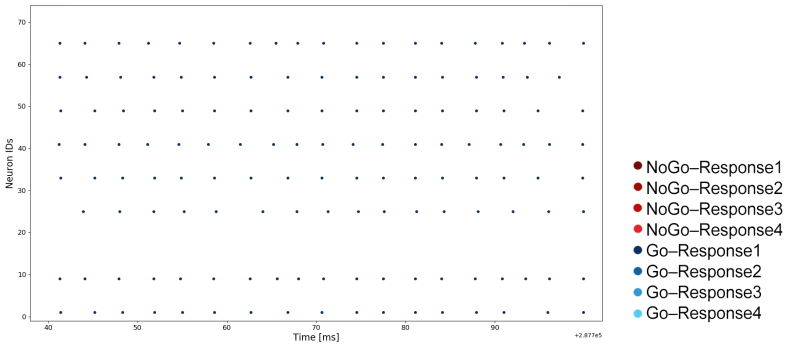

Figure 18: **Trial 400 minus phase (2).** Striatal activations in the minus phase of trial 400. For the Go-Response1 neurons involved, activity is steadily enhanced compared to the early stage and differs a little from the half stage.

In the plus phase of trial 400, thalamus and cortical excitation and GPi inhibition are firmly substantial (Figure 19).

Striatal activity (in Figure 20) for Go-Response1) does not differ much from the frequency already obtained in the half stage (in Figure 16 for Go-Response1); it is not surprisingly since the system has reached a steady behaviour. Eventually, note that striatal activations in the minus phase (Figure 18) regard only neurons of Go-Response1 module. Learning is achieved.

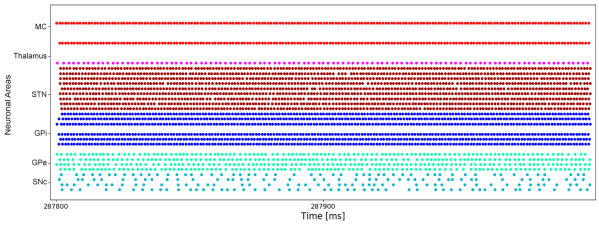

(a)

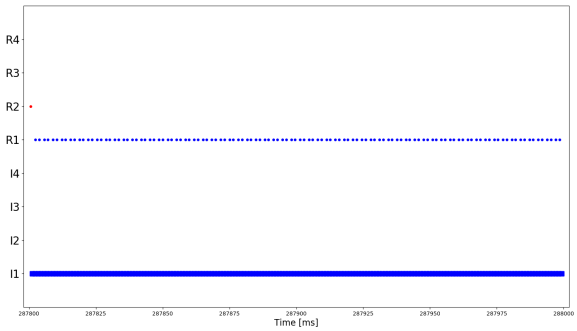

(b)

Figure 19: **Trial 400 plus phase (1).** (a) The network activations in the plus phase of trial 400. thalamus and cortical excitation and GPi inhibition are firmly substantial. (b) Input/output activations.

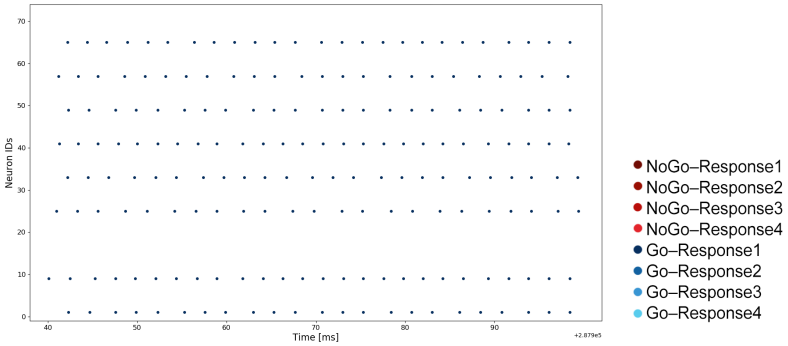

Figure 20: **Trial 400 plus phase (2).** Striatal activations in the plus phase of trial 400. At steady state, Go-Response1 activations are pretty the same in the minus phase and the plus phase.

A set of experiments was conducted to analyse the behaviour of the network to achieve a statistical significance. Figure 21 reports the learning curve of the neural network in physiological conditions. The model is able to learn the correct SR associations in about 40 epochs, using the parameters in Appendix A.4.

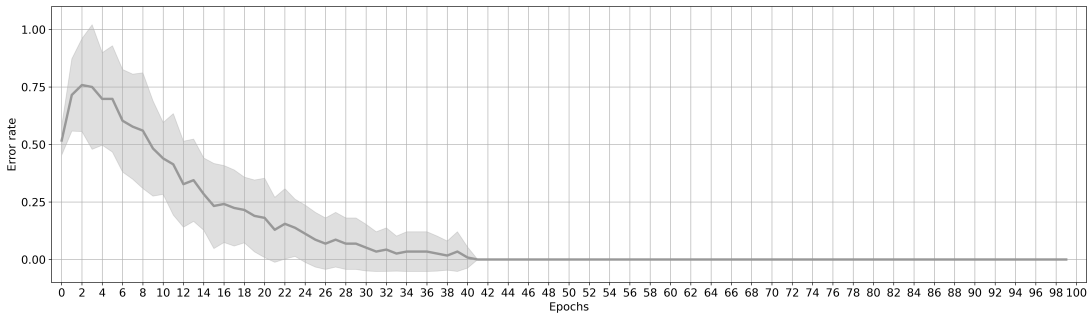

Figure 21: **Physiological condition learning curve.** Learning curves of the neural network in physiological conditions, averaged over 30 networks, trained for 100 epochs.

4.3 Motor learning in pathological conditions

Pathological conditions have been obtained by damaging the network in different ways. We will first describe current knowledge of physiological lesion in PD and the connection with possible simulated lesion in the network, broadly speaking, leading to a first set of simulations. Then, we are going to cover clinical knowledge about lesion entities, extracting a logic within the experimental context, which drives a second set of simulations. Eventually, we will show the damaged network behaviour obtained by the simulations, providing results in great detail, divided per groups.

4.3.1 Dopaminergic neurons lesion

Aggregation of misfolded proteins has been suggested to be the characteristic feature of the neurodegenerative process, despite it is not clear whether Lewy bodies (LBs) are causes or scars of neurodegeneration. In particular, α-synuclein (AS) is a protein abundant in DA neurons and is the protein chiefly considered responsible for the formation of LBs. It is thought to lead to toxicity when aggregated into pathological oligomers, fibrils and LBs, but the precise mechanism whereby it leads to toxicity and cell death remains obscure, since the relationship of AS aggregation and dopaminergic degeneration is unclear. Several *in vitro* and *in vivo* studies suggested that AS can spread from cell to cell and from region to region, which dramatically promotes PD pathogenesis and progression [16].

Also, the normal physiological structure and function of AS still remain unclear. Accumulating evidence shows that the molecule is involved in multiple steps related to DA metabolism, including DA synthesis, storage, release, and uptake. The regulatory effect of AS on DA metabolism is likely to tone down the amount of cytoplasmic DA at nerve terminals. Then, aggregations of AS leads to disrupted homeostasis of dopamine metabolism, increased cytoplasmic DA levels and enhanced oxidative stress in dopaminergic neurons [17, 18, 19, 20].

In conclusion, what is clear is that LBs formation in dopaminergic neurons (presynaptic terminals) slow down DA metabolism, slowly toning down the amount of DA in the striatum (postsynaptic terminals). From this point, the aim is that of simulating the reduction of the amount of DA in the striatum.

We consider that the reduction of DA can be achieved implementing different kind of lesions in NEST. Precisely, there are three types of lesion:

lt.1 cut dopaminergic neuron connection,

lt.2 decrease weight synapse connection between SNc and striatum,

lt.3 decrease dopaminergic neurons firing rate

Simulating PD by lesioning the network in any of the three cases means to reduce dynamic range of the DA signal. Dynamic range is critical for learning appropriate Go/NoGo representations from error feedback, as network weights are adjusted on the basis of difference in activity states in the two phases of network settling. Because tonic DA levels are low, PD networks have an overall propensity for NoGo learning, but the dynamic range of phasic dips during negative feedback is reduced. Go learning is degraded because limited amounts of available DA reduce the potency of phasic bursts, activating less of a Go representation during positive feedback.

The lesion of **lt.1** is the only one provided by Emergent and is both the less similar to the neurophysiology and the sharpest in terms of damage of the three types. The lesion of **lt.2** impacts the firing rate of dopaminergic neurons indirectly and reduces the amount of DA which reaches the striatum (further weakening the learning of Go signals), whereas **lt.3** acts directly on the firing rate.

A first disease investigation is the exploration of all the three lesions listed above, by making a trade-off between resources and granularity, then fictional lesion parameters, in order to evaluate the impact of the degree of a damaged parameter over the network behaviour. Nevertheless, given the knowledge about the extent of the possible lesions to SNc, a wiser and more accurate experimentation can be set up, taking a look at clinical findings.

4.3.2 The underlying ratio

Currently, the literature still falls far short of a uniform and well-defined view of PD disease development, neither of diagnosis and treatment.

Ugrumov claims that according to the last classification, three stages are distinguished in PD development: (i) the preclinical stage — from the onset of neurodegeneration to the appearance of nonmotor

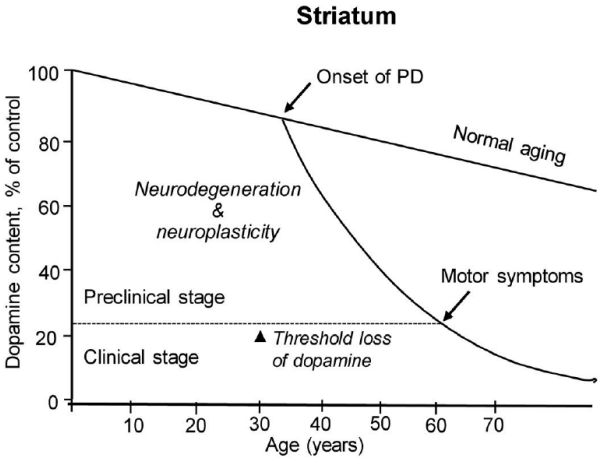

Figure 22: **Schematic representation of the pathogenesis of PD in patients.** The manifestation of progressive degradation of the nigrostriatal dopaminergic system in patients with PD as a loss of DA in the striatum to a threshold level, which is associated with the onset of motor disorders. Reproduced from [20, Figure 1A].

symptoms, (ii) the prodromal stage — from the onset of nonmotor symptoms to the appearance of motor symptoms, bradykinesia, rigidity, rest tremor, (iii) clinical stage — from the appearance of motor symptoms to death. PD develops up to 30 years at the preclinical stage without manifestations of motor disorders. They appear after a "threshold" degradation of the nigrostriatal dopaminergic system at a loss of 70% dopamine in the striatum (refer to Figure 22) and 50-60% dopaminergic neurons in the SN (not reported) [20].

Grosch et al. [21] claim that the loss of dopaminergic striatal nerve terminals at motor symptoms onset is rather difficult to determine, reporting a comparison between different studies performing regression analysis to the onset of motor symptoms to estimate the proportion of lost striatal and putaminal dopaminergic terminals, which goes from 39% to 51% for striatum and 51% to 71% for the putamen.

Cheng et al. [22] suggest that at the time of first diagnosis of PD, only 30% or so of dopaminergic neurons have been lost and 50-60% of their axon terminals. Moreover, they conclude that at the time of motor symptom onset the extent of loss of striatal dopaminergic markers exceeds that of SN dopamine neurons, in accordance with Ugrumov. This conclusion is consistent with observations that, at the time of death, depending on disease duration, while there has been 60-80% loss of SN dopamine neurons there has been a much more profound loss of striatal or putaminal dopaminergic markers.

Lastly, findings indicate that degeneration of dopaminergic neurons in PD is not total even after many years of illness [23] and at the time of death.

Which stages should be investigated?

The low efficacy of treating patients is due to the late diagnosis and start of therapy, after the degeneration of most specific neurons and depletion of neuroplasticity. It is believed that the development of early diagnosis (ED) and preventive treatment will delay the onset of specific symptoms. The current methodology for the development of ED is based on searching biomarkers, such as premotor symptoms.

In this direction, handwriting is currently considered a potential powerful marker for ED of PD, with the purpose of building tailored intelligent systems to support clinicians based on machine learning techniques [24, 25, 26, 27]. Handwriting, indeed, is one of the abilities that is affected by PD; because of that, researchers investigate the possibility of using handwriting alterations, caused by the disease, as diagnostic signs, expression of small entity of SN lesion, in the early stage of the disease, before the onset of evident symptoms. This hypothesis is well-founded and based on the fact that in the clinical practice there is already employed a writing exam for the diagnosis of neuropsychological deficits, employed also for PD, which comprises asking the patient to create a series of specific drawings; specifically, they are the *Clock drawing test* and *Sketching a spiral*, which are now commonly used in clinic. Despite this, though, no specific writing test has been approved or indicated in the guidelines of clinical practice for PD diagnosis. Nevertheless, these studies show that, even when the clinical diagnosis is at an early stage (based on UPDRS) and subjects do not show obvious motor deficits, the analysis of the dynamic characteristics (such as speed, acceleration, fluence) associated with a fine motor task, such as the generation of writing,

already allows to highlight some differences between healthy subjects and patients. PD patients are also known to have motor learning difficulties [28]. Consequently, the execution of a *new* motor task is more deficient than the execution of a *known* motor task. Furthermore, it has been shown that there are similarities between the dynamic characteristics of the writing movements of healthy subjects when they produce a motor task new to them and those measured in subjects who have a PD in the early stage [27].

Therefore, it may be of interest to investigate the learning deficits shown by the model for different stages of dopaminergic degeneration in order to have some indications on the possibility of developing a protocol (involving the execution and learning of new motor tasks) that would be simple to perform, inexpensive and non-invasive and, thus, allows for early detection of the onset of the disease.

With this in mind, further experiments have been set up, taking into consideration both the results obtained in the first set of experiments, to enhance the sensitivity of the behaviour of the network to further perturbations, and the thresholds here reported, implying them as a guide to choose lesion percentage, with the aim of investigating, of course, the preclinical stage, for the ED. Moreover, this refined set of lesion has been simulated to occur at early stage of learning, half stage of learning and after learning.

4.3.3 Simulated dopamine depletion

All the simulations have been carried out for 50 epochs since, as showed in Figure 21, stable learning is achieved around 50 epochs; then, 50 epochs has been labeled as the time required for the network to complete learning. This choice has been adopted both for the experiments concerning lesions applied at early stage of learning and for the others. The experiments carried out over 5–10 networks suffer from low statistical power in accordance with the law of large numbers, but were needed to evaluate whether the simulated entity of the lesion caused learning perturbation within the maximum learning time; in other words, the sensitivity extent to perturbation. This choice is the resulting trade-off between time available for research and the computational complexity of completing a single trial, given the intent of this investigation. Thus, we will report the results obtained in those experiments and the considerations leading to the following, crucial, experimental research.

Lesion type 1 Lesion type 1 implies to cut dopaminergic neuron connection. It has been simulated the death of 25%, 50%, 75%, 100% neurons of SNc, at early stage of learning over 10 networks. Results are not reported graphically because they are not statistically significant, but provide guidance on how to adjust the model.

Indeed, it appears that no significant difference exist with respect to physiological behaviour, also when the lesion is 75%. Learning is impaired when dopaminergic neurons are fully disconnected, since the learning curve shows that responses are being randomly chosen. Then, results are consistent with motor learning impairment without the DAergic system, but they suggest that the chosen parameters involve the nigrostriatal synapse to have a very strong net effect on the reward process, since it is expected an alteration in the behaviour after the cut of two neurons.

Lesion type 2 Lesion type 2 means to reduce the weight of the nigrostriastal connection gradually, for 1, 2, 3 and 4 neurons. The weight has been simulated being adjusted to 0.2, 0.15, 0.1 and 0.05 for SNc-Go and twice the value for SNc-NoGo. This type of lesion is the one with highest granularity; then, due to time limits, training has been carried over only 5 networks, therefore results have very low statistical power. Therefore, the aim is to investigate how learning behaviour changes by damaging the synapse weight, within the maximum time of 50 epochs; thus, learning time and other quantitative parameters are not statistically significant due to the very small number of networks simulated in accordance with the law of large numbers.

Given the small number of experiments, no meaningful gains were achieved with small adjustment of the parameter with respect to the physiological case, sign also of robustness of the implementation. A satisfactory outcome is appreciable by comparing the learning curves of 0.05 synapse weight for an increasing number of damaged neurons (Figure 23). Indeed, as neurons are gradually damaged, learning velocity is slowing down, since the curve is slowly degrading, although neither time or other quantitative parameters are to be considered statistically significant; by means of activations, striatal neurons are less excited by SNc. In the last case (d), learning stagnates to an error other than zero, oscillating around 25%. It means that the effect of the damaged DAergic system plus the effect of the other afferents to striatal activity is such that, on average, one response fails to be learnt.

This trial proves that the network being simulated is robust to parameters perturbations and that they need to be adjusted to increase the sensitivity towards disturbance and to obtain significant change in behaviour for simulating DA depletion.

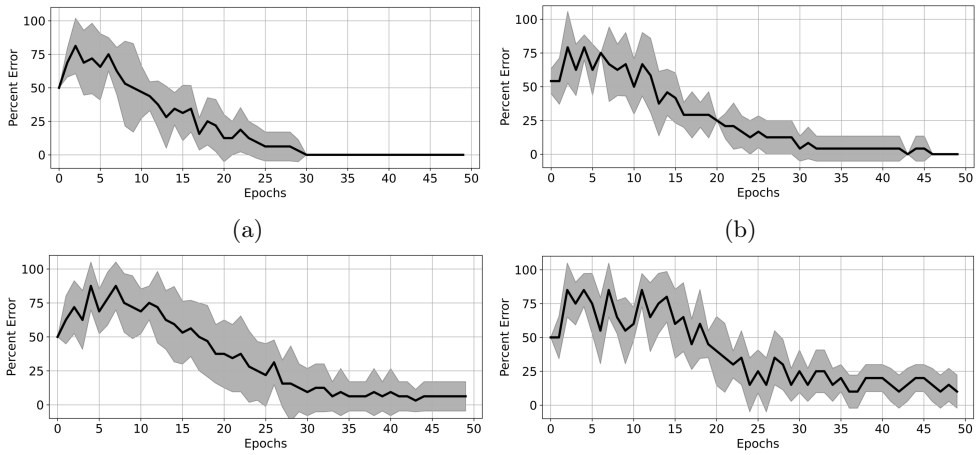

Figure 23: **Lesion type 2.** Reduced synapse strength. (a) 1 damaged neuron. (b) 2 damaged neurons. (c) 3 damaged neurons. (d) 4 damaged neurons.

Lesion type 3 Lesion type 3 is the reduction of the firing rate of dopaminergic neurons. Here too, the behaviour proved to be the same as in physiological conditions for small reductions of the parameter.

In short, the set of experiments hitherto presented intended to explore the capacity of the model and of the tool (NEST) in the space of parameters. At this point, we have gathered the appropriate knowledge of the framework built up and we are able to launch purposeful trials.

Further lesion Given the clinic remarks reported, a set of experiments inspired by clinic observations is developed, taking into account the findings of the other experiments. Then, the synapse weight has been reduced to 0.15 and the starting firing rate has been set to 1000 spikes/sec.

From this point, the firing rate has been reduced by 0.2, 0.3, 0.5, 0.7, 0.8 and 0.9, in order to simulate, in a way, DA content reduction of 20%, 30%, 50% and so on. It must be pointed out that such an experiment does not claim to establish a complete matching with the physiology.

Learning curves are reported in Figures 24–25 for damaged networks with the occurrence of the lesion at early stage, half stage and after learning.

Early stage Further investigation of the behaviour at early stage was considered analysing the average activations for striatal neurons in the plus phase of the column corresponding to the correct response, in the simulation time. The analysis showed that, with the advance of learning, the rate of activity, on average, for a neuron in the Go column of the correct response is likely to increase; moreover, this activity is sufficiently greater than zero because of DA. Thus, the evolution of the striatal activity as the network is incrementally damaged reports, as expected, that the rate is slightly moving downward from the setpoint after depletion is 50%.

Figure 24 may be read considering 20%-30% up to 50%-60% as a simulation of preclinical stage and from 70% on motor symptoms and clinical stage. In (a) and (b) learning is slowed with respect to the physiological behaviour (refer to Figure 21) but a descending error trend is maintained. In (c) learning is slowed more with respect to (b); (d) learning is thoroughly impaired, losing the descending trend, in accordance with motor symptoms. In (e) and (f) learning is impaired, in accordance with the advanced stage of the disease. The fact that learning is slowed down only after 50% lesion is coherent with Frank's findings [2].

After the results obtained in this experimentation, object of further analysis is the quantity of simulated DA depletion which did slow down learning at early stage, yet preserving the descending trend, *small lesions*, which do not produce evident misbehaviour but may generate altered parameters, in line with the considerations about ED based on deteriorated behaviour in handwriting.

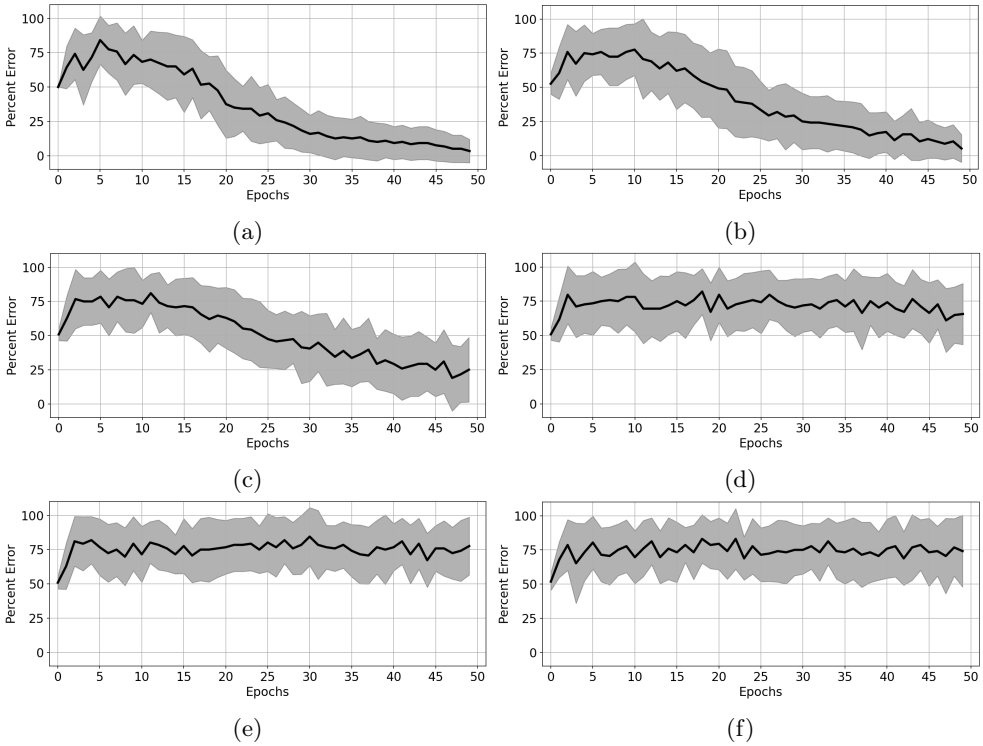

Figure 24: **Further investigation of lesion type 3 - early stage.** Learning curves of 30 networks for each subgroup, trained over 50 epochs. We report here the correspondence between DA depletion and the value of firing rate: (a) 20%: 800.0 spikes/s, (b) 30%: 700.0 spikes/s, (c) 50%: 500.0 spikes/s, (d) 70%: 300.0 spikes/s, (e) 80%: 200.0 spikes/s, (f) 90%: 100.0 spikes/s.

Half stage Then, to continue our experimentation, the lesion of firing rate has been applied at half stage of learning, which is 25th epoch and only the 30%, 50% and 70% have been considered, as they represent preclinical stage in our context. This means that learning continues from the 25th epoch of the learning process of the physiological network.

Looking at the behaviour of the network in physiological conditions (Figure 21), at half stage the network is completing to learn one response, on average. Results in Figure 25 show that the behaviour of the damaged network is slightly deteriorated roughly similarly whether the entity of lesion is smaller or larger (from 30% (a) to 70% (c)).

The reason why motor learning is not being completed has been discovered by analysing the activations of the modules of the network within each simulation. Indeed, NoGo learning has proceeded, leading to disinhibition of GPe neurons but, above all, STN is overexcited, leading to the disinhibition of GPi in the response time window of the simulation and not to select the response. The activity of STN is in the form of occasional bursts, which cause the impairment of learning. STN bursts have been linked to PD: microrecordings of the STN suggest that the high level of STN neuronal activity with irregular and bursty pattern is associated to parkinsonian rigidity and akinesia, whereas periodic oscillatory bursts are associated to parkinsonian tremor [29].

After stage Eventually, the lesion of the firing rate has been applied after learning, which is 50th epoch and only the 30%, 50% and 70% have been considered. At this stage of learning, we point out that BG response is consolidated by the strengthening of corticostriatal synapses, the physiological error is at steady-state and learning is dependent more on cortical than striatal learning.

The Figure 25 (b) shows that with 30% lesion the network succeeds in giving all the correct answers steadily, (d) with 50% lesion errors occur but variance is low and (f) with 70% the variance is even higher. It is consistent with the findings that PD patients are able to continue performing already learnt motor tasks, although not smoothly. In fact, parkinsonian tremor tends to decrease or disappear with the performance of a voluntary movement.

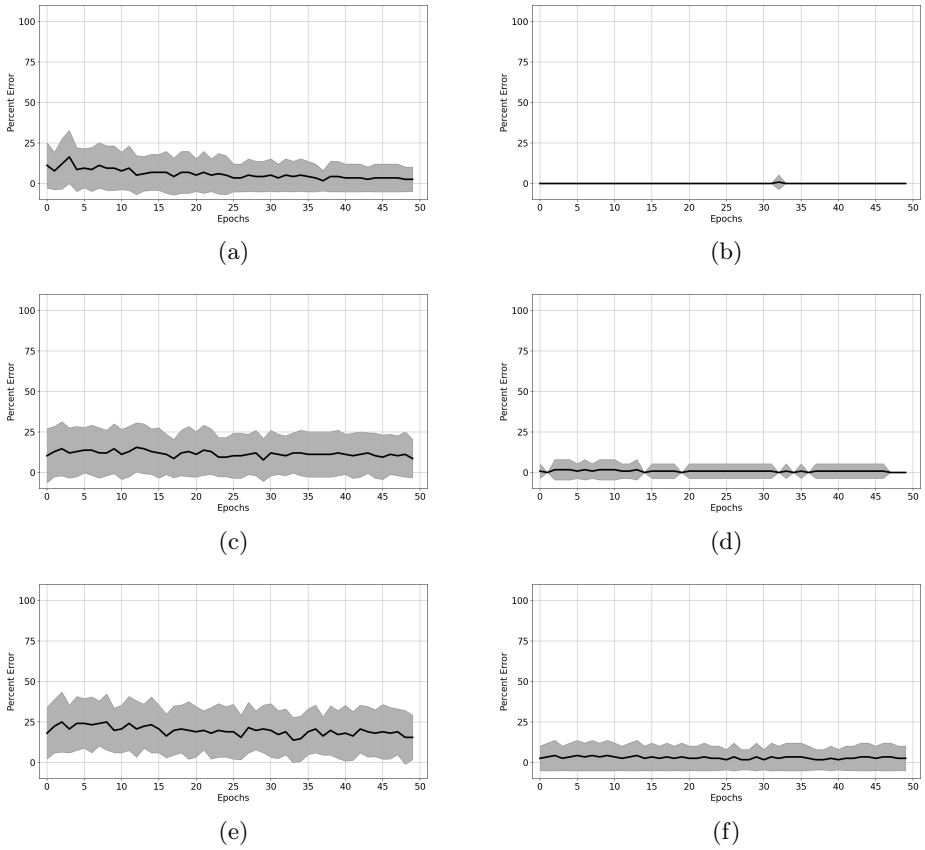

Figure 25: **Further investigation of lesion type 3 - half and after learning stage.** Learning curves of 30 networks for each subgroup, trained over 50 epochs. Half stage: (a) 30% DA depletion: 700.0 spikes/s firing rate. (c) 50% DA depletion: 500.0 spikes/s firing rate. (e) 70% DA depletion: 300.0 spikes/s firing rate. After learning stage: (b) 30% DA depletion: 700.0 spikes/s firing rate. (d) 50% DA depletion: 500.0 spikes/s firing rate. (f) 70% DA depletion: 300.0 spikes/s firing rate.

5 Conclusions

Parkinson's disease (PD) affects millions of people worldwide and its treatment and evolution is closely tied to the time of diagnosis. Considering that, in general, PD is diagnosed after the degeneration of most dopaminergic neurons, it is important to develop support systems for the early diagnosis (ED). Handwriting is one of the abilities that is affected by neurodegenerative diseases, including PD. For this reason, researchers investigate the possibility of using the handwriting alterations caused by the disease as diagnostic signs. In this sense, is it possible to develop a strategy leading to early diagnose PD?

The approach adopted to address the question is a model-based engineering one. Since PD is characterized by the death of dopaminergic neurons in the SNc and the impairment of motor task learning, a neurocomputational model is designed and developed and the acquisition of novel motor skills is simulated; moreover, experiments simulating different degrees of damage are carried out in order to understand if, on the basis of the behaviour of the model, deficits in learning can be identified also for minor lesions.

The model provided does not differentiate between different parts of the striatum and simulates reward process as simple DA bursts and dips, not addressing the brain mechanisms which cause phasic bursts and dips during positive and negative feedback. It is remarkable, on the other hand, that inhibitory connections inside the striatum, the effect of interneurons, have been introduced in the architecture of the network, despite at a high level of abstraction. In other words, the current model the BG, including DA and interneurons, provides a working hypothesis that can be tested experimentally and behaviourally.

The behaviour of the network in learning a novel motor task has been analyzed, evaluating the neural activations within the network, the error rate of the responses and the robustness of the network to small perturbations of the parameters. Results obtained fit those reported by many neuroimaging and experimental studies presented in the literature [1].

Further experiments have been carried out to simulate neurodegenerative disorders, namely PD,

damaging the network in varying degrees. First of all, results obtained by these experiments validate the hypothesis that the BG play a key role during learning. Furthermore, the deteriorated performance in handwriting tasks, found in the experimental studies on PD patients, is echoed in the deteriorated learning behaviour of the network when damaged by minor lesions. The engineering impact of these findings is that some symptoms, motor learning symptoms, actually arise in the simulated network before the evident motor symptoms. Specifically, the mean learning curves, show that 20% DA depletion already causes a degradation of the performance with respect to the network behaviour in physiological conditions in learning a novel motor skill; indeed, while in physiological conditions the network is able to complete learning within the 50th epoch of simulation, conversely, damaging by 20% DA content, learning decelerates and does not become steady either at the 50th epoch, thereby confirming that learning symptoms arise at early stage of the disease. We may assume that the error would reach steady-state within a larger number of epochs, but we have not conducted this experimentation for resource constraints. In other words, we can claim that with 20% DA depletion in the network, learning is not impaired, but the dynamic properties of learning are different with respect to the physiological case. It should be noted that this result is achieved by means of another bio-inspired technique in the field of AI, computational modeling, as an alternative to the handwriting analysis and handwritten pattern recognition, confirming their results and taking a step further.

First of all, the other techniques have proved that discriminating between unhealthy and healthy subjects on the basis of simple and easy-to-perform handwriting tasks is possible, but they are based on data from patients already diagnosed with PD. Instead, this work proves that there may exist abnormalities of motor learning process, due to alterations in the dynamics of BG functionality, which do not yet involve the presence of symptoms typical of the confirmed diagnosis, because the network shows having some difficulties in motor learning already with 20% DA depletion, damage that does not cause symptoms that normally lead to diagnosis.

Furthermore, considering that the feature of parkinsonian movements is that PD patients are not able to properly develop a motor plan, made of properly synchronized smaller elementary movements to execute a more complex sequence of movements in such a way as to minimize energy consumption and to execute a motor task smoothly [26], the performed movement will be composed of many stop-and-go, interspersed with properly synchronized movements whose extent decreases as the size of the lesion increases. In other words, PD patients are not able to learn the complex movement and they segment it into pieces. It means that, in the early stage of the disease, the feature of the deteriorated motor plan does not concern the shape of the handwriting, rather the dynamics and the variations in acceleration. Specifically, the study proves that these variations in acceleration concern the dynamics of learning a novel motor task and are not found in the execution of already learnt tasks.

Now, as motor learning results in smooth handwriting, in PD patients this process is not complete, thus the handwriting movements are jerky; this feature can be studied by analysing velocity and acceleration profile of handwriting. What emerges from this study is that a higher value of normalized jerk, the time-derivative of acceleration, and abrupt changes in movement velocity and acceleration during the dynamics of novel motor learning, may result also for patients not yet diagnosed PD with respect to healthy subjects, while so far it has been proved only for patients already diagnosed with PD.

Then, the research reveals that while many features in the literature concern the shape of the handwriting, actually it is not as important as the dynamic producing that shape, which may be measured by velocity and acceleration.

In summary, results obtained with the current damaged network provides a working feedback for the hypothesis of deteriorated behaviour in motor learning task, as handwriting, at the early stage of the disease, that can be further tested experimentally and behaviourally at different scales. And not only that. Findings give an indication that subjects should be tested on the execution of novel and relatively complex motor tasks and that velocity and acceleration profiles of this task should be evaluated to differentiate between healthy and non healthy undiagnosed subjects for an ED.

Funding

This research received no external funding.

Conflicts of Interest

The authors declare no conflict of interest.

A Appendices

A.1 The hypothesised motor learning theory

The hypothesis we accept in this paper for motor learning theory [1] is the following: acquiring a new motor skill requires two phases, in which two different processes occur. The early stage of learning is more related to the acquisition of the sequence of point to reach and this process is performed by the BG (through the caudate nucleus, one of the structures that make up the corpus striatum). Simultaneously, the cerebellar cortex starts to acquire an internal model of the skill. As learning proceeds, the activation is confined to a specific area of the cerebellar cortex and increased activity in the dentate nucleus reflects the acquired internal model of the skill.

Consequently, the process that allows humans to acquire a novel motor skill can be divided into two distinct phases:

- Early in learning, task performance is more dependent on the procedural knowledge maintained by the cortex-basal ganglia system. During the learning stage, humans learn the spatial sequence associated to the motor task in visual coordinates, i.e. the sequence of points to reach in order to realize the task.
- After long-term practice, task performance is more dependent on the motor sequence maintained by the cortex-cerebellar system. During the automatic stage, the sequence of motor commands in motor coordinates is acquired and comes to be executed as a single behaviour.

It goes without saying that object of the research presented here is the first phase, the learning stage.

A.2 Neuronal model

Biological neuron models, also known as spiking neuron models, are mathematical descriptions of the properties of certain cells in the nervous system that generate sharp electrical potentials across their cell membrane, roughly one millisecond in duration, called action potentials or spikes. Since spikes are transmitted along the axon and synapses from the sending neuron to many other neurons, spiking neurons are considered to be a major information processing unit of the nervous system. In the literature, many neuron models have been developed to deal with different levels of abstraction, which goes hand in hand with model complexity. The more granular the empirical content is modelled, the greater the model complexity is. Simplified models are useful for analysis and study of large interconnected networks, whereas detailed descriptions involving thousands of coupled differential equations are useful for channel-level investigation. Spiking neuron models can be divided into different categories: the most detailed mathematical models are biophysical neuron models (also called Hodgkin-Huxley models) that describe the membrane voltage as a function of the input current and the activation of ion channels. Mathematically simpler are integrate-and-fire (IF) models that describe the membrane voltage as a function of the input current and predict the spike times without a description of the biophysical processes that shape the time course of an action potential. Even more abstract models only predict output spikes as a function of the stimulation where the stimulation can occur through sensory input or pharmacologically.

In short, the non-leaky IF is based on the representation of a neuron as an electric RC circuit. The leaky IF model, instead, contains, compared to the non-leaky integrate-and-fire model a "leak" term in the membrane potential equation, reflecting the diffusion of ions through the membrane. In other words, neuron models where action potentials are described as events are called IF models. No attempt is made to describe the shape of an action potential.

NEST allows to choose between different types of neuronal models at different levels of abstraction. The IF neuron model is one of the most widely used models for analyzing the behavior of neural systems. Indeed, the model has become established as a canonical model for the description of spiking neurons because it is capable of being analyzed mathematically while at the same time being sufficiently complex to capture many of the essential features of neural processing.

This is the reason why, the neuronal model adopted in this work is the conductance-based (synapses) leaky IF neuron model provided by NEST. In this model, the incoming spikes induce a post-synaptic change in conductance modeled by an exponential function, normalized in such a way that a pre-synaptic spike of unit weight results in a conductance peak of 1 nS. The choice of this model fits perfectly well with the aim of characterizing the neurons according to the parameters of interest, while maintaining a high level of abstraction considered the complexity of the neuronal network. In particular, all the neurons of the BG of the proposed model are of the same nature, whose parameters are reported in Table 1. This

hypothesis is borrowed from Frank's work [2, 3], in which a similar neural behavior is hypothesized for all the neuronal populations considered.

	C_m $[pF]$	g_L $[nS]$	τ_{inh} $[ms]$	τ_{exc} $[ms]$	V_{th} $[mV]$	V_{reset} $[mV]$
IF neuron	2.0	0.2	10.0	0.5	-40.0	-70.0

Table 1: **Neuronal parameters.** C_m capacity of the membrane; g_L leak conductance; τ_{inh} rise time constant of the inhibitory synaptic alpha function; τ_{exc} rise time constant of the excitatory synaptic alpha function; V_{th} potential threshold; V_{reset} reset potential of the membrane.

A.3 Learning algorithms

Synaptic connection weights were trained using a reinforcement learning version of Leabra, which is more biologically plausible than standard error backpropagation. To simulate feedback effects, the learning algorithms involve two distinct phases: *minus* and *plus phase*. In the *minus phase*, the network settles into activity states based on input stimuli and its synaptic weights, ultimately choosing a response. In the *plus phase*, the network resettles in the same manner, with the only difference being a change in simulated dopamine release (i.e: SNc activity) depending on the selected response: dopaminergic neurons increase from tonic to phasic (i.e: high) level of activity, which means that the unit firing rate goes from 0.5 to 1.0 for a correct response, whereas an incorrect response causes a decrease to zero level of activity, meaning from rate of 0.5 to 0.

The learning rule adopted in the BG to change synaptic connection weights is inspired by the version of reinforcement learning rule of the Leabra framework implemented in Emergent [4]. For learning, Leabra uses a combination of error-driven and Hebbian learning. In short, the error-driven component computes a simple difference of a pre- and post- synaptic activation product across the two phases. For Hebbian learning, Leabra uses essentially the same learning rule used in competitive learning. The error-driven and Hebbian learning components are combined additively at each connection to produce a net weight change.

The equation for the Hebbian weight changes adopted is:

$$\Delta_{hebb} w_{ij} = x_i^+ y_j^+ - y_j^+ w_{ij} = y_j^+ (x_i^+ - w_{ij}) \tag{3}$$

where x is the presynaptic activation, y the postsynaptic activation and $-/+$ represents minus/plus phase, respectively. The equation for error-driven task learning is:

$$\Delta_{err} w_{ij} = (x_i^+ y_j^+) - (x_i^- y_j^-) \tag{4}$$

which is subject to a soft-weight bounding to keep within the 0–1 range:

$$\Delta_{sberr} w_{ij} = [\Delta_{err}]_+ (1 - w_{ij}) + [\Delta_{err}]_- w_{ij} \tag{5}$$

The two terms are then combined additively:

$$\Delta_{w_{ij}} = \epsilon [k_{hebb}(\Delta_{hebb}) + (1 - k_{hebb})(\Delta_{sberr})] \tag{6}$$

where ϵ represents the learning rate parameter and k_{hebb} is a parameter that controls the associated proportion of the two types of learning.

A.4 Implementation parameters

The model parameters of the connections between the Basal Ganglia, Motor Cortex and Thalamus are reported in Tables 2–3–4–5–6–7.

Layer	Size	Neuronal model	Synapse model
Striatum	72	IF	exc/inh
GPe	4	IF	inh
GPi	8	IF	exc/inh
STN	9	IF	exc/inh
SNc	4	IF	-
Thalamus	4	IF	exc/inh
MC	8	IF	exc
Input	18	IF	-
Output	4	IF	exc

Table 2: **Network layers.** Size is in terms of the number of neurons; IF is conductance-based leaky integrate-and-fire neuron model (details in A.2); exc stands for excitatory, inh for inhibitory synapse.

Presynaptic Layer	Postsynaptic Layer	Model	Synapse			Delay	Conn.
			Dist	Weight Mean	Var		
Input	Striatum	exc	Uniform	0.07	0.05	1.0	a2a
Striatum	Striatum	inh	Uniform	0.03	0.02	1.0	a2a
MC	Striatum Go	exc	Uniform	0.45	0.05	1.0	col
MC	Striatum NoGo	exc	Determ.	1.0		1.0	col
SNc	Striatum Go	exc	Determ.	0.15		1.0	col
SNc	Striatum NoGo	inh	Determ.	0.3		1.0	col
Striatum Go	GPi	inh	Determ.	1.5		1.0	col
Striatum NoGo	GPe	inh	Determ.	1.0		1.0	col
GPe	GPi	inh	Determ.	1.0		1.0	col
STN	GPi	inh	Determ.	6.0		1.0	a2a
GPe	STN	inh	Determ.	0.35		1.0	a2a
MC	STN	exc	Uniform	0.65	0.2	1.0	a2a
Input	MC	exc	Uniform	0.05	0.005	3.0	a2a
Thalamus	MC	exc	Determ.	2.0		1.0	col
MC	Thalamus	exc	Determ.	1.5		1.0	col
GPi	Thalamus	inh	Determ.	1.0		1.0	col
MC	Output	exc	Determ.	2.0		1.0	col

Table 3: **Basal ganglia synapses parameters.** The synapses parameters are: the neuronal model, the weight is characterized by numerical distribution, mean and variance, the delay and the connectivity rule, which can be all to all (a2a) or by columns (col).

Layer	Weight	Rate $[spikes/s]$	Decay law
Input	0.1	500.0	No
MC	1.0	500.0	No
GPi	1.0	16000.0	No
GPe	1.0	4000.0	No
SNc tonic	1.0	500.0	No
SNc phasic burst	1.0	1000.0	No
SNc phasic dip	1.0	0.0	No
MC response	1.0	1000.0	No
STN	4.0	9000.0	Yes

Table 4: **NEST generators parameters.**

Parameter	Value	Description
Time window (Tw)	Variable	Duration of the minus phase.
Tw step size	$2ms$	Step of simulation of the minus phase.
Tw min time	$400ms$	Minimum time of simulation.
Tw max time	$800ms$	Maximum time of simulation.
Tw spiking activity	$60ms$	Subsection of Tw in which the firing activity is computed for each output neuron.
Threshold spiking activity	0.25	The firing rate; calculated as the #of spikes/Tw spiking activity.

Table 5: **Minus phase parameters.**

Parameter	Value	Description
Time window (Tw)	$200ms$	Duration of the plus phase.
Striatal learning Tw	$60ms$	Subsection of Tw in which the firing activity is computed in striatal learning.
Cortical learning Tw	$60ms$	Subsection of Tw in which the firing activity is computed in cortical learning.
Eps striatal LTD	0.01	Learning rate for LTD in striatal learning.
Eps striatal LTP	0.1	Learning rate for LTP in striatal learning.
K hebb striatal	0.01	Constant for hebbian learning in striatal learning.
Eps cortical	0.00001	Learning rate in hebbian cortical learning.

Table 6: **Plus phase parameters.**

Parameter	Value	Description
w_i	4.0	Initial weight
w_f	0.6	Final weight
$rate_i$	9000.0	Initial rate
$rate_f$	2000.0	Final rate
t_i	0	Initial time [trials]
t_f	400	Final time [trials]
τ_{intra}	800/3	Time constant intra trial exponential decay of weight parameter
c_i	2.0	Initial time constant inter trial
c_f	0.6	Final time constant inter trial
τ_{inter}	120/3	Time constant inter trial exponential decay of weight parameter

Table 7: **STN decay law parameters.**

References

[1] I. Gigi, R. Senatore, and A. Marcelli, "Neurocomputational modeling of the basal ganglia in motor learning at mesoscopic scale: an overview," Sep 2021. [Online]. Available: engrxiv.org/9ftwd

[2] M. J. Frank, "Dynamic dopamine modulation in the basal ganglia: a neurocomputational account of cognitive deficits in medicated and nonmedicated parkinsonism," *Journal of cognitive neuroscience*, vol. 17, no. 1, p. 51–72, 2005.

[3] ——, "Hold your horses: a dynamic computational role for the subthalamic nucleus in decision making," *Neural Networks*, vol. 19, pp. 1120–1136, 2006.

[4] R. O'Reilly, B. Aisa, and B. Mingus, "The emergent neural modeling system," *Neural Networks*, vol. 21, no. 8, p. 1146–1152, 2008.

[5] T. Fardet, S. B. Vennemo, J. Mitchell, H. Mørk *et al.*, "Nest 2.20.0," 01 2020.

[6] C. B. Holroyd and M. G. H. Coles, "The neural basis of human error processing: reinforcement learning, dopamine, and the error-related negativity," *Psychological Review 109*, vol. 109(4), p. 679–709, Oct 2002.

[7] B. Ballanger, T. van Eimeren, E. Moro, A. M. Lozano *et al.*, "Stimulation of the subthalamic nucleus and impulsivity: release your horses," *Annals of neurology*, vol. 66, no. 6, p. 817—824, December 2009.

[8] R. Senatore, "The role of basal ganglia and cerebellum in motor learning. a computational model," Ph.D. dissertation, Università degli studi di Salerno, 2012.

[9] M. Lindahl and J. Hellgren Kotaleski, "Untangling basal ganglia network dynamics and function: Role of dopamine depletion and inhibition investigated in a spiking network model," *eNeuro*, vol. 3, no. 6, 2016.

[10] W. Gerstner, W. M. Kistler, R. Naud, and L. Paninski, *Neuronal Dynamics: From Single Neurons to Networks and Models of Cognition*. USA: Cambridge University Press, 2014.

[11] D. Z. Jin, N. Fujii, and A. M. Graybiel, "Neural representation of time in cortico-basal ganglia circuits," *Proceedings of the National Academy of Sciences*, vol. 106, no. 45, pp. 19 156–19 161, 2009.

[12] E. Navarro-López, U. Çelikok, and N. Şengör, "A dynamical model for the basal ganglia-thalamocortical oscillatory activity and its implications in parkinson's disease," 2020.

[13] J. Lee, T. R. Darlington, and S. G. Lisberger, "The neural basis for response latency in a sensorymotor behavior," *bioRxiv*, 2019.

[14] A. Blenkinsop, S. Anderson, and K. Gurney, "Frequency and function in the basal ganglia: the origins of beta and gamma band activity," *The Journal of Physiology*, vol. 595, no. 13, pp. 4525–4548, 2017.

[15] K. Gurney, T. Prescott, and P. Redgrave, "A computational model of action selection in the basal ganglia. ii. analysis and simulation of behaviour," *Biological cybernetics*, vol. 84, pp. 411–23, 07 2001.

[16] L. Xu and J. Pu, "Alpha-synuclein in parkinson's disease: From pathogenetic dysfunction to potential clinical application," *Parkinson's Disease*, vol. 2016, pp. 1–10, 08 2016.

[17] S. Yu, K. Uéda, and P. Chan, "Alpha-synuclein and dopamine metabolism," *Molecular neurobiology*, vol. 31, p. 243–254, Feb 2005.

[18] M. Huber, L. Beyer, C. Prix, S. Schönecker *et al.*, "Metabolic correlates of dopaminergic loss in dementia with lewy bodies," *Movement Disorders*, vol. 35, no. 4, pp. 595–605, 2020.

[19] J. Galvin, "Interaction of alpha-synuclein and dopamine metabolites in the pathogenesis of parkinson's disease: a case for the selective vulnerability of the substantia nigra," *Acta neuropathologica*, vol. 112, pp. 115–26, 09 2006.

[20] M. Ugrumov, "Development of early diagnosis of parkinson's disease: Illusion or reality?" *CNS Neuroscience & Therapeutics*, vol. 26, 06 2020.

[21] J. Grosch, J. Winkler, and Z. Kohl, "Early degeneration of both dopaminergic and serotonergic axons – a common mechanism in parkinson's disease," *Frontiers in Cellular Neuroscience*, vol. 10, 12 2016.

[22] H.-C. Cheng, C. Ulane, and R. Burke, "Clinical progression in parkinson disease and the neurobiology of axons," *Annals of neurology*, vol. 67, pp. 715–25, 06 2010.

[23] R. Djaldetti, M. Lorberboym, Y. Karmon, T. Treves *et al.*, "Residual striatal dopaminergic nerve terminals in very long-standing parkinson's disease: A single photon emission computed tomography imaging study," *Movement disorders : official journal of the Movement Disorder Society*, vol. 26, pp. 327–30, 02 2011.

[24] L. S. Bernardo, A. Quezada, R. Munoz, C. R. Pereira *et al.*, "Handwritten pattern recognition for early parkinson's disease diagnosis," *Pattern Recognition Letters*, vol. 125, pp. 78–84, 2019.

[25] D. Impedovo, G. Pirlo, and G. Vessio, "Dynamic handwriting analysis for supporting earlier parkinson's disease diagnosis," *Information (Switzerland)*, vol. 9, 10 2018.

[26] R. Senatore and A. Marcelli, "A paradigm for emulating the early learning stage of handwriting: Performance comparison between healthy controls and parkinson's disease patients in drawing loop shapes," *Human Movement Science*, vol. 65, 04 2018.

[27] R. Senatore, A. Marcelli, R. De Micco, A. Tessitore *et al.*, "Handwriting as a diagnostic tool for the early detection of parkinson's disease," 2021.

[28] M. Olson, T. Lockhart, and A. Lieberman, "Motor learning deficits in parkinson's disease (pd) and their effect on training response in gait and balance: A narrative review," *Frontiers in Neurology*, vol. 10, 02 2019.

[29] A. Benazzouz, S. Breit, A. Koudsie, P. Pollak *et al.*, "Intraoperative microrecordings of the subthalamic nucleus in parkinson's disease," *Movement Disorders*, vol. 17, no. S3, pp. S145–S149, 2002.